NACA TN No. 1449

NATIONAL ADVISORY COMMITTEE FOR AERONAUTICS

TECHNICAL NOTE

No. 1449

THEORETICAL SUPERSONIC WAVE DRAG OF UNTAPERED SWEPTBACK AND RECTANGULAR WINGS AT ZERO LIFT

By Sidney M. Harmon

Langley Memorial Aeronautical Laboratory
Langley Field, Va.

Washington
October 1947

NATIONAL ADVISORY COMMITTEE FOR AERONAUTICS

TECHNICAL NOTE NO. 1449

THEORETICAL SUPERSONIC WAVE DRAG OF UNTAPERED SWEPTBACK AND RECTANGULAR WINGS AT ZERO LIFT

By Sidney M. Harmon

SUMMARY

A theoretical investigation of the supersonic wave drag at zero lift of a series of untapered sweptback wings having thin symmetrical biconvex parabolic-arc sections has been presented in NACA TN No. 1319. The investigation has been extended to include Mach numbers which bring the Mach line behind the wing leading edge and also to include wings of rectangular plan form. The results are presented in a unified form so that a single chart permits the direct determination of the wave drag for this family of wings over an extensive range of sweepback angle, Mach number, aspect ratio, and thickness ratio. The results obtained for the total wave drag of the sweptback wings are applicable to the same family of wings having a corresponding degree of sweepforward.

When the Mach line lies behind the wing leading edge, the wave-drag coefficients of the sweptback and rectangular wings are shown to reach maximum values at certain limiting aspect ratios and remain constant for all aspect ratios greater than these limiting values. The limiting aspect ratio is equal to $\frac{2 \cot \Lambda}{\cot \Lambda \sqrt{M^2 - 1} - 1}$ for the sweptback wing and to $\frac{1}{\sqrt{M^2 - 1}}$ for the rectangular wing, where Λ is the angle of sweepback and M is the Mach number. The variation of wing wave-drag coefficient with Mach number over the complete range of supersonic Mach number is shown to become less pronounced with decreasing aspect ratio. It is also shown that sweepback obtained by rotating the wing panels rearward can give appreciable reductions in wing wave-drag coefficient at all supersonic speeds.

INTRODUCTION

Recent developments in airfoil theory for supersonic speeds (references 1 to 3) indicate pronounced effects of sweepback and

aspect ratio on the drag. In reference 3, a method based on thin-airfoil theory for a frictionless fluid (reference 2) was applied to calculate the supersonic wave drag at zero lift for a series of wings having thin symmetrical biconvex parabolic-arc sections with untapered plan forms and various angles of sweepback and aspect ratios. The results in reference 3, however, are limited to those cases in which the Mach line lies ahead of the wing leading edge, or to a range of Mach number from 1.0 to the value equal to the secant of the angle of sweepback. The term "Mach line" as used herein refers to the Mach wave that originates at the leading edge of the center section, unless specified otherwise.

The present paper extends the calculations of reference 3 for the same series of wings in order to present wave-drag results for cases in which the Mach line lies behind the wing leading edge. These data are obtained for wings of rectangular and sweptback plan forms and cover an extensive range of Mach number beginning with the value at which the Mach line coincides with the wing leading edge. In order to present a more complete picture, the results of reference 3 that cover the lower range of Mach number are reproduced herein together with additional curves computed from formulas given in reference 3. The results of the entire investigation are presented in a unified form similar to that given in reference 3 so that the wave drag for this family of wings may be determined directly from a single chart over an extensive range of sweepback angle, Mach number, aspect ratio, and thickness ratio. In the Tenth Annual Wright Bros. Memorial Lecture given on December 17, 1946, Dr. von Kármán indicated that at zero lift the total wave drag for a sweptforward wing is identical with that obtained for the same wing having a corresponding amount of sweepback. The results of the present investigation for the total drag of sweptback wings, therefore, are applicable to the same family of wings having a corresponding amount of sweepforward. The distributions of section drag, however, will differ in the two cases. Although the calculations have been made for the biconvex parabolic-arc profile, the data may be applied to indicate corresponding results for profiles similar to the biconvex parabolic-arc profile.

SYMBOLS

x, y, z	coordinates of mutually perpendicular system of axes
c	chord of airfoil section, measured in flight direction
t/c	thickness ratio of section, measured in flight direction
Λ	angle of sweep, degrees

$m = \cot \Lambda$

h	wing semispan measured along y-axis, semichords except in appendix A
K	parameter indicating spanwise position equal to y/m, semichords
A	aspect ratio $\left(\frac{4h^2}{S}\right)$
S	wing area
l/t	slenderness ratio, ratio of wing semispan measured along midchord station to maximum thickness of center section
V	velocity in flight direction
u	x-component of disturbance velocity, positive in flight direction
$\bar{u}$	disturbance velocity caused by source line with reversal in sign of m
I	source factor required to maintain a given wedge angle
$\frac{dz}{dx}$	slope of airfoil surface
R.P.	real part of complex expression
M	Mach number
$\beta = \sqrt{M^2 - 1}$	
y_a	coordinate measured along y-axis which is shifted to tip section, semichords
y_b	coordinate measured along y-axis which is shifted to opposite tip section, semichords
c_{d_∞}	section wave-drag coefficient without tip effect
c_d	section wave-drag coefficient including tip effect
Δc_d	increment in section wave-drag coefficient caused by wing tips
Δc_{d_I}	increment in section wave-drag coefficient caused by wing tip located on same half of wing as section

$\Delta c_{d_{II}}$ increment in section wave-drag coefficient on one wing panel caused by tip of opposite wing panel

C_{D_∞} wing wave-drag coefficient without tip effect

C_D wing wave-drag coefficient including tip effect

ΔC_D increment in wave-drag coefficient caused by tips, complete wing

$\Delta C_{D_{II}}$ increment in wave-drag coefficient on one wing panel caused by tip of opposite wing panel, complete wing

ξ, η coordinates which replace x and y, respectively, used to indicate origin of source line

w' w in transformed coordinate system of reference 2

Primed values of A, y, y_a, y_b, h, z, and m indicate transformation involving multiplication by factor β.

Subscript notations for u and $\frac{dz}{dx}$ indicate the origin of source line in terms of coordinates x and y, respectively.

ANALYSIS

Basic data.- The analysis is based on thin-airfoil theory for small pressure disturbances relative to the ambient pressures. The axes used are the mutually perpendicular x, y, z system in which the x-axis is taken in the direction of flight positive to the rear, the y-axis is along the span positive to the right, and the z-axis is positive upwards. The symbols used to designate the wing-planform parameters are shown in figure 1. The analysis is made for untapered sweptback and rectangular wings of biconvex parabolic-arc profile at zero lift. The wing is considered to be cut off in a direction parallel to the direction of flight. The Mach numbers considered in this analysis correspond to those for which the Mach line lies behind the wing leading edge, that is, for Mach numbers greater than the secant of the angle of sweepback $\left(m > \frac{1}{\beta}\right)$.

Theory.- The present analysis corresponds essentially to that given in reference 3 where $m \leqq \frac{1}{\beta}$. By following the analysis of reference 3, the section wave-drag coefficient for the symmetrical biconvex parabolic-arc profile at the spanwise station y is

$$c_d(y) = \frac{16\frac{t}{c}}{Vc^2} \int_{y/m}^{\frac{y}{m}+c} \left(\frac{c}{2} - x + \frac{y}{m}\right) u \, dx \qquad (1)$$

where u refers to either surface of the airfoil.

The evaluation of equation (1) involves the determination of the disturbance velocity u at each point on the wing. An appropriate system of semi-infinite source and sink lines which represent the wings considered herein is given in appendix A. Appendix A also gives the u-expressions for these source lines and their regions of influence on the wing as determined by the Mach cones from their extremities. These regions of influence for the individual source lines are illustrated in figure 2 and are given in table I as the limits of the variables of integration for x along the chord and for y along the span.

Figure 2 is given in order to illustrate typical Mach lines for Mach numbers in which the Mach wave from the nose lies behind the wing leading edge $\left(m > \frac{1}{\beta}\right)$. Inasmuch as the wing cut-off is represented by reversed semi-infinite source-line distributions (appendix A), the tip Mach cones in figure 2 for the various aspect ratios show the extent of the region of the tip effect. For $A > \frac{2m}{m\beta + 1}$, the tip effect on the wing is influenced only by the adjacent tip. If $A < \frac{1}{\beta}$, both wing tips influence each wing panel.

Formulas for section wave-drag coefficients.- The formulas for the section wave-drag coefficients for sweptback and rectangular wings, which result from the integration of the u-expressions in equation (1), are presented in appendix B. These formulas give expressions for section wave-drag coefficient without the tip effect c_{d_∞} and also the expressions for the increments in section wave-drag coefficient caused by the wing tips Δc_d.

Wave-drag coefficients for complete wing.- The formulas for the wave-drag coefficients for untapered sweptback and rectangular wings of biconvex parabolic-arc profile are given in appendix B.

RESULTS AND DISCUSSION

Variation of section wave-drag coefficient along span.- Figures 3 and 4 show the variation of section wave-drag coefficient c_d along the span for the wings of 45° and 0° sweepback, respectively.

The results are shown in figure 3(a) for the 45° sweptback wing of infinite aspect ratio, that is without the tip effect, at several Mach numbers. The lowest Mach number 1.41 represents a case in which the Mach line is coincident with the wing leading edge. In this case, as noted in reference 3, the wing has a very high drag and the section wave-drag coefficient increases in the outboard direction and approaches infinity at an infinite distance from the wing center. As noted later in this section the assumptions of the linearized theory may be violated at a Mach number of 1.41 except for very thin wings.

For the higher Mach number of 1.50, the ordinates are reduced in magnitude and the spanwise variation of c_{d_∞} is markedly flatter. The section wave-drag coefficient without tip effect c_{d_∞} has a minimum value at the center section, increases in the outboard direction, and then approaches a constant finite value. This constant value of c_{d_∞} results from the fact that if the effect of the wing tips is neglected, the flow is two-dimensional over the parts of the wing ahead of the Mach wave from the vertex. The component parallel to the wing leading edge has no effect here; that is, this region is influenced only by the component of the velocity normal to the wing leading edge (reference 4). The pressures, therefore, are exactly those that would be computed by the Ackeret theory of linearized two-dimensional supersonic flow by use of the normal velocity component (reference 5). Outboard of the point where the Mach wave from the vertex intersects the wing trailing edge, the flow is entirely two-dimensional. In this region, therefore, the section wave-drag coefficient based on all parameters measured normal to the wing leading edge has the constant Ackeret value for an infinite rectangular wing. The value is:

$$c_{d_{\infty n}} = \frac{16}{3\beta_n}\left(\frac{t}{c}\right)_n^2 \qquad \text{(See appendix B, equation (B4).)}$$

where the subscript n indicates that c_{d_∞}, β, and t/c are measured normal to the wing leading edge. The section wave-drag measured normal to the wing leading edge is obtained from this section wave-drag coefficient, and the component of this force in the flight direction gives the true section drag. As a result there is obtained

$$c_{d_\infty} = c_{d_{\infty n}} \cos^3 \Lambda = \frac{16\left(\frac{t}{c}\right)_m^2}{3\sqrt{m^2\beta^2 - 1}}$$

When this value for c_{d_∞} is compared with the Ackeret result for an infinite rectangular wing having the same thickness ratio in the flight direction, c_{d_∞} in the region of two-dimensional flow is found to increase because of sweepback by the factor $\frac{m\beta}{\sqrt{m^2\beta^2 - 1}}$.

The highest Mach number 2.24 represents a case in which the wing is well outside the Mach cone. At this Mach number, c_{d_∞} approaches the two-dimensional value at a comparatively small distance outboard of the center section.

In figure 3(b), the spanwise distributions of c_d are shown for the 45° sweptback wing at a Mach number of 1.8 for various aspect ratios. The aspect ratios in this figure were selected so that they represent each of the different types of tip effects. (See fig. 2.)

A comparison of the c_{d_∞}-distributions illustrated in figure 3(a) with those given in figure 2(a) of reference 3 shows an important difference between the conditions where the Mach line lies ahead of the wing leading edge $\left(m < \frac{1}{\beta}\right)$ and where the Mach line lies behind the leading edge $\left(m > \frac{1}{\beta}\right)$. If $m < \frac{1}{\beta}$, the section wave-drag coefficient without tip effect c_{d_∞} decreases to zero at some point along the span, then becomes negative, and finally approaches zero asymptotically at infinity; whereas if $m > \frac{1}{\beta}$, c_{d_∞} does not decrease to zero with increasing values of y but approaches a constant positive value. The contributions of the adjacent tip effect to the shape of the c_d-distribution Δc_{d_I} are similar for both $m > \frac{1}{\beta}$ and $m < \frac{1}{\beta}$. This may be seen by taking the difference of the c_d-curves for $A = \infty$ and $A = 5$ in figure 3(b) and comparing the resulting distribution with Δc_{d_I} given in figure 2(b) of reference 3.

The increment in section wave-drag coefficient on one wing panel caused by the tip of the opposite wing panel $\Delta c_{d_{II}}$, however, tends to be shifted inboard when the Mach number is increased from the range $m < \frac{1}{\beta}$ to $m > \frac{1}{\beta}$. (Note Mach lines from opposite tip in fig. 2(a) of this paper and $\Delta c_{d_{II}}$ in fig. 2(b) of reference 3.) This comparison indicates, therefore, that in general for a given sweepback angle and comparatively high aspect ratios in which $\Delta c_{d_{II}}$ is zero $\left(A > \frac{2m}{m\beta + 1}\right)$ or very small, an increase in the Mach number

which brings the Mach line behind the leading edge of the wing appears to result in a shift of the center of pressure of the wave drag in the outboard direction.

The results are shown in figure 4(a) for the rectangular wing of infinite aspect ratio at several Mach numbers. These results correspond to the Ackeret theory, which shows a constant section wave-drag coefficient along the span.

The results are given in figure 4(b) for the rectangular wing at a Mach number of 1.25 for several aspect ratios. The aspect ratios in this figure, as in figure 3(b), were selected so as to represent each of the different types of tip effects. (See fig. 2.)

Effect of tips on wing wave-drag coefficient.- The present analysis for $m > \frac{1}{\beta}$ indicated, as noted in reference 3 for $m < \frac{1}{\beta}$, that the integrated value of Δc_{d_I} over the wing is zero if the aspect ratio is equal to or greater than $\frac{2m}{m\beta + 1}$. Inasmuch as $\Delta C_{D_{II}}$ is zero for $A \geqq \frac{2m}{m\beta + 1}$ (see fig. 2(a)), the total increment in wave-drag contributed by the tip is zero if $A \geqq \frac{2m}{m\beta + 1}$.

For the rectangular wing, $m = \infty$ and the total increment in C_D caused by the tips is zero if the aspect ratio $A \geqq \frac{1}{\beta}$. (See appendix B, equation (B11).) In the range $A \geqq \frac{1}{\beta}$, therefore, the wave-drag coefficient for the rectangular wing is independent of aspect ratio and is equal to the Ackeret result for a two-dimensional wing. If the aspect ratio for the rectangular wing is less than $1/\beta$, the increment in C_D caused by the tips is found to be negative.

Generalized curves for wing wave-drag coefficient.- Figures 5 to 8 present generalized curves for determining the wing wave-drag coefficient over an extensive range of sweepback angle, Mach number, aspect ratio, and thickness ratio. The results are given in figures 5 and 6 for the sweptback wings. As noted previously in the "INTRODUCTION," the data in these figures are applicable to the same family of wings having a corresponding amount of sweepforward. The results for the rectangular wing are presented in figures 7 and 8.

The data in figures 5 to 8 apply specifically to untapered wings at zero lift with biconvex parabolic-arc profiles and the wing tips cut off in the direction of flight. The results, however, may be applied to indicate approximate results for profiles similar to

the biconvex parabolic-arc profile. Because of the assumptions of the present linearized theory, the results presented herein for Mach numbers in the vicinity of sec Λ or at very high Mach numbers are in general questionable, except for small or vanishingly small thickness ratios, inasmuch as the calculated pressure disturbances over the wing at such Mach numbers tend to be large relative to the ambient pressures. For applications to very small aspect ratios, the present theory may require some modifications.

The results in figures 5 and 6 for the sweptback wing are given in terms of the wave-drag-coefficient parameter $\frac{C_D \tan \Lambda}{100\left(\frac{t}{c}\right)^2}$, the Mach number parameter $\cot \Lambda \sqrt{M^2 - 1}$, and the aspect ratio parameter $A \tan \Lambda$. As shown in reference 3, these parameters group the variables C_D, Λ, A, M, and t/c in a unified form and thereby permit the direct determination of the drag coefficient from a single chart over an extensive range of sweepback angle, Mach number, aspect ratio, and thickness ratio. For a 10-percent-thick 45° sweptback wing, the drag-coefficient parameter in figures 5 and 6 becomes simply C_D, the aspect-ratio parameter, A, and the Mach number parameter, $\sqrt{M^2 - 1}$. The results in figures 5 and 6 may be applied to any sweepback angle covering a range of aspect ratio from 0 to 10 cot Λ and a range of Mach number from 1 to $\sqrt{1 + 49 \tan^2 \Lambda}$.

The results in figures 5(a) and 5(b) refer to Mach numbers corresponding to $\cot \Lambda \sqrt{M^2 - 1}$ equal to or less than 1; that is, where the Mach line lies ahead of the wing leading edge. These data represent results which were obtained directly from figure 5 of reference 3 with several additional curves which were calculated from the formulas given in reference 3. The results in figures 5(c) and 5(d) refer to Mach numbers corresponding to $\cot \Lambda \sqrt{M^2 - 1}$ equal to or greater than 1; that is, where the Mach line lies behind the wing leading edge. These data were calculated from the formulas given in appendix B of the present paper. The data in figure 6 were obtained by cross-plotting the results in figure 5; therefore, the range of Mach number and aspect ratio in figure 6 is the same as that given in figure 5.

Effect of aspect ratio and Mach number on wing wave-drag coefficient for sweptback wings.- If the Mach line is well ahead of the wing leading edge, increasing the aspect ratio in the range $A \gtrapprox \cot \Lambda$ reduces C_D (see fig. 5(a)); however, for all aspect ratios where the Mach line approaches the wing leading edge and also for $A \lessapprox \cot \Lambda$ for Mach numbers $\cot \Lambda \sqrt{M^2 - 1} \leq 1$, C_D is reduced with decreasing aspect ratio.

If the Mach line lies behind the wing leading edge, the wing wave-drag coefficient reaches a maximum value which is constant for all aspect ratios greater than a certain limiting value $\left(A \gtrsim \frac{2m}{m\beta - 1}\right)$.

Figure 6 indicates that in general the variation of C_D over the complete range of Mach number becomes less pronounced as the aspect ratio is decreased. For $A \lesssim \cot \Lambda$ the variation of C_D with M is comparatively small.

Effect of aspect ratio and Mach number on wing wave-drag coefficient for rectangular wings.- Figures 7 and 8 indicate the effects of aspect ratio and Mach number on C_D for rectangular wings. Figure 7 shows the variation of $\frac{C_D}{100\left(\frac{t}{c}\right)^2}$ with aspect ratio for constant Mach numbers. The wing wave-drag coefficient reaches a maximum value at an aspect ratio equal to $1/\sqrt{M^2 - 1}$ and remains constant for higher values of aspect ratio.

Figure 8 shows the variation of $\frac{C_D}{100\left(\frac{t}{c}\right)^2}$ with Mach number M for constant aspect ratios. When the aspect ratio is equal to or greater than 1, C_D is independent of aspect ratio for Mach numbers equal to or greater than 1.41. The curves in figure 8 indicate that the variation of C_D over the complete range of Mach number becomes less pronounced as the aspect ratio is reduced; thus, the same trend noted previously for the sweptback wings is shown.

Effect of sweepback angle on wing wave-drag coefficient.- In order to study the effect of sweepback on the wing wave drag, the method of obtaining the sweepback must be considered. In the present investigation, wing wave-drag results have been obtained for two different methods of increasing the sweepback angle, and the data are presented in figures 9 and 10.

In the first method of obtaining sweepback, the data for which is given in figure 9, the sweepback angle is increased by rotating the wing rearward about a vertical axis at the midpoint of the center section. The root and tip sections of the rotated wing are then modified so that they become parallel to the flight direction in order to conform to the family of sweptback wings considered herein. For this method, the aspect ratio and the thickness ratio in the flight direction are reduced with increasing sweepback, but the wing area and slenderness ratio are maintained constant. The slenderness ratios in figure 9 are based on a thickness ratio of 0.10 measured in a direction normal to the wing leading edge. The thickness ratio t/c

measured in the flight direction, therefore, varies with sweepback as $\cos \Lambda$ or is equal to $0.1 \cos \Lambda$. The aspect ratio is reduced with sweepback by the factor $\cos^2 \Lambda$. The aspect ratio A is related to the slenderness ratio l/t by the following formula:

$$A = 0.2 \frac{l}{t} \cos^2 \Lambda$$

The results in figure 9 indicate that if the wing is sweptback by rotation on the basis of constant l/t, sweepback can give appreciable reductions in the wave-drag coefficient at all supersonic speeds.

For the second method of obtaining sweepback, the data for which is shown in figure 10, the sweepback angle is increased by sliding the sections rearward. For this method, the aspect ratio, the thickness ratio in the flight direction, and the wing area are maintained constant. The results in figure 10 indicate that if the wing is sweptback by sliding the sections rearward, sweepback can give appreciable reductions in wave-drag coefficient only at Mach numbers for which the forward Mach line is well ahead of the wing leading edge. At Mach numbers, however, for which the forward Mach line approaches the wing leading edge or is behind it $\left(\cot \Lambda \sqrt{M^2 - 1} \gtrsim 0.95\right)$, wing sweepback obtained with constant A and t/c increases the wave-drag coefficient.

CONCLUDING REMARKS

The theoretical investigation of the supersonic wave drag of untapered sweptback wings at zero lift has been extended to include Mach numbers which bring the Mach line behind the wing leading edge and to include wings of rectangular plan form. The wing sections investigated were biconvex, composed of two parabolic arcs, and the wing tips were considered to be cut off in the direction of flight. The following conclusions have been drawn:

Mach line ahead of the wing leading edge:

1. If the Mach line is well ahead of the wing leading edge, increasing the aspect ratio in the range of aspect ratio greater than or approximately equal to the cotangent of the angle of sweepback reduces the wing wave-drag coefficient.

2. For aspect ratios less than approximately the cotangent of the angle of sweepback and for all aspect ratios where the Mach line approaches the wing leading edge, the wing wave-drag coefficient decreases with decreasing aspect ratio.

Mach line behind the wing leading edge:

3. The wave-drag coefficient of the sweptback wing reaches a maximum value at an aspect ratio for which the Mach line from the leading edge of the center section intersects the trailing edge at the tip; this maximum coefficient remains constant for higher values of aspect ratio.

4. The wave-drag coefficient of the rectangular wing reaches a maximum value at an aspect ratio for which the Mach line from the leading edge of the tip section intersects the trailing edge of the tip on the opposite wing panel; this maximum coefficient remains constant at higher values of aspect ratio.

5. The wave-drag coefficient of all wings for all aspect ratios decreases with increasing Mach number.

Complete range of Mach number:

6. With a comparatively high aspect ratio, an increase in the Mach number which moves the Mach line behind the wing leading edge appears to move the center of pressure of the wave drag in the outboard direction.

7. The variation of the wing wave-drag coefficient with Mach number over the complete range of supersonic Mach number becomes less pronounced as the aspect ratio is decreased.

8. Sweepback obtained by rotating the wing panels rearward can give appreciable reductions in the wave-drag coefficient at all supersonic speeds.

9. Sweepback obtained by sliding each section rearward can give appreciable reductions in wave-drag coefficient only when the Mach line is well ahead of the wing leading edge. When the Mach line approaches the wing leading edge or is behind it, sweepback obtained by sliding each section rearward increases the wing wave-drag coefficient.

Langley Memorial Aeronautical Laboratory
National Advisory Committee for Aeronautics
Langley Field, Va., July 10, 1947

APPENDIX A

FORMULAS FOR u-EXPRESSIONS AND INTEGRATION LIMITS FOR INTEGRAND IN EQUATION (1) FOR UNTAPERED SWEPTBACK AND RECTANGULAR WINGS OF BICONVEX PARABOLIC-ARC PROFILE AT ZERO LIFT $\left[m = \cot \Lambda \geq \frac{1}{\beta}\right]$

Sweptback Wings

The desired integrand u in equation (1) is determined in a manner similar to that described in appendix A of reference 3. The sweptback wing of desired profile shape and plan form is built up by superposition of the solutions obtained for a semi-infinite oblique wedge. On the basis of the linearized theory, reference 2 derives a solution representing an oblique semi-infinite (sweptback) source line making the angle of sweepback Λ with the y-axis. The solution utilized for the pressure field or for the disturbance velocity is

$$u_{0,0} = \text{R.P. } I \cosh^{-1} \frac{x - m\beta^2 y}{\beta|y - mx|} \tag{A1}$$

where the subscript notation indicates that the source line starts at the origin of coordinates ($x = 0$, $y = 0$). Equation (A1) is shown in reference 2 to satisfy the boundary condition for a thin oblique wedge making the half-angle $\left(\frac{dz}{dx}\right)'$ in the transformed coordinate system of reference 2 ($y' = y\beta$, $z' = z\beta$), where $\left(\frac{dz}{dx}\right)' = \frac{w'}{V} = I \frac{\pi}{V} \frac{\sqrt{1 - m'^2}}{m'}$. The source factor I in terms of the physical coordinate system required to maintain the desired wedge is shown in reference 3 to be represented by

$$I = \frac{V}{\pi} \frac{m}{\sqrt{1 - m^2\beta^2}} \frac{dz}{dx}_{(0,0)} \tag{A2}$$

If the source line is swept ahead of the Mach line, $m\beta > 1$, then substitution of equation (A2) in equation (A1) gives

$$u_{0,0} = \text{R.P.} - \frac{iVm}{\pi\sqrt{m^2\beta^2 - 1}} \left(\frac{dz}{dx}\right)_{0,0} \cosh^{-1} \frac{x - m\beta^2 y}{\beta\left|y - mx\right|}$$

$$= \frac{Vm}{\pi\sqrt{m^2\beta^2 - 1}} \left(\frac{dz}{dx}\right)_{0,0} \cos^{-1} \frac{x - m\beta^2 y}{B\left|y - mx\right|} \qquad \text{(A3)}$$

The sweptback wing of biconvex parabolic-arc profile is represented by the following system of elementary semi-infinite oblique source lines: Source lines of equal strength are placed along the leading and trailing edges beginning at the center section in conjunction with a constant distribution of sink lines along the chord also beginning at the center section. At the tip, where the wing is cut off, reversed semi-infinite source and sink lines are distributed so as to cancel exactly the effect of those originating at the center section in the entire region of space outboard of the tip.

For $m > \frac{1}{\beta}$, the sources which are considered to originate at the wing trailing edge have no effect on the wing because their Mach lines are behind the wing. (See fig. 2(a).) The disturbance velocity u is then expressed in the following form (reference 3, appendix A, equation (A1)):

$$u = u_{0,0} + \bar{u}_{0,0} - \frac{1}{D}u_{0,0} - \frac{1}{D}\bar{u}_{0,0}$$

$$- u_{h/m,h} - \bar{u}_{h/m,-h} + \frac{1}{D}u_{h/m,h} + \frac{1}{D}\bar{u}_{h/m,-h} \qquad \text{(A4)}$$

where the subscript notation indicates the origin of the source line. The bars over u refer to the source lines caused by the opposite wing panel; that is, $\bar{u}$ indicates a source line with a reversal in the sign of m.

In equation (A4), the u-expressions are given by the real parts of the following expressions:

$$u_{\xi,\eta}(x, y) = \frac{Vm}{\pi\sqrt{m^2\beta^2 - 1}} \left(\frac{dz}{dx}\right)_{\xi,\eta} \cos^{-1} \frac{x - \xi - m\beta^2(y - \eta)}{\beta\left|y - \eta - m(x - \xi)\right|} \qquad \text{(A5)}$$

$$\bar{u}_{\xi,\eta}(x, y) = \frac{Vm}{\pi\sqrt{m^2\beta^2 - 1}} \left(\frac{dz}{dx}\right)_{\xi,\eta} \cos^{-1} \frac{x - \xi + m\beta^2(y - \eta)}{\beta\left|y - \eta + m(x - \xi)\right|} \qquad \text{(A6)}$$

where ξ,η represents the origin of the elementary source lines. For the biconvex parabolic-arc profile,

$$\left(\frac{dz}{dx}\right)_{\xi,\eta} = 2\frac{t}{c}$$

The symbol $\frac{1}{D}$ in equation (A4) refers to an integration which represents the influence of a uniform distribution of source lines along the chord of the biconvex profile beginning at the position ξ,η. This integration is expressed as (reference 3, appendix A, equation (A2)):

$$\frac{1}{D}u_{\xi,\eta}(x, y) = \int_{x-\beta|y-\eta|}^{\xi} \frac{dI}{d\xi'} \cosh^{-1} \frac{x - \xi' - m\beta^2(y - \eta)}{\beta|y - \eta - m(x - \xi')|}\, d\xi'$$

$$= -\frac{V(y - \eta)}{\pi} \frac{d^2z}{dx^2} \left\{ \cosh^{-1} \frac{x - \xi}{\beta|y - \eta|} - \frac{1}{\sqrt{m^2\beta^2 - 1}} \left[1 - \frac{m(x - \xi)}{y - \eta}\right] \cos^{-1} \left| \frac{\frac{x - \xi}{\beta(y - \eta)} - m\beta}{1 - \frac{m(x - \xi)}{y - \eta}} \right| \right\} \quad \text{(A7)}$$

where ξ' is the variable of integration representing the ξ-coordinate of the origin of each source line in the distribution of source lines. For the biconvex profile,

$$\frac{d^2z}{dx^2} \approx -\frac{4}{c}\left(\frac{t}{c}\right)$$

Equation (A7) is expressed as a function of $\frac{x - \xi}{y - \eta}$; that is,

$$\frac{1}{D}u_{\xi,\eta}(x, y) = (y - \eta)\, f\left(\frac{x - \xi}{y - \eta}\right)$$

Then

$$\frac{1}{D}\bar{u}_{\xi,\eta}(x, y) = -(y - \eta)\, f\left[\frac{x - \xi}{-(y - \eta)}\right]$$

Rectangular Wings

For the rectangular wing, $m = \infty$ and the following expressions result from substituting $m = \infty$ in equation (A5), (A6), and (A7):

$$u_{\xi,\eta}(x, y) = \frac{V}{\pi\beta}\frac{dz}{dx}\left[\pi - \cos^{-1}\frac{\beta(y-\eta)}{x-\xi}\right]$$

$$\bar{u}_{\xi,\eta}(x, y) = \frac{V}{\pi\beta}\frac{dz}{dx}\cos^{-1}\frac{\beta(y-\eta)}{x-\xi}$$

$$\frac{1}{D}u_{\xi,\eta}(x, y) = -\frac{V}{\pi}(y-\eta)\frac{d^2z}{dx^2}\left\{\cosh^{-1}\frac{x-\xi}{\beta|y-\eta|} + \frac{1}{\beta}\left(\frac{x-\xi}{y-\eta}\right)\left[\pi - \cos^{-1}\frac{\beta(y-\eta)}{x-\xi}\right]\right\}$$

$$= (y-\eta)\,f\left(\frac{x-\xi}{y-\eta}\right)$$

$$\frac{1}{D}\bar{u}_{\xi,\eta}(x, y) = -(y-\eta)\,f\left[\frac{x-\xi}{-(y-\eta)}\right]$$

Limits of Integrations

The limits of integration with regard to x for the section wave-drag coefficients and with regard to y for the total wing wave-drag coefficients are discussed. The u-components caused by each of the elementary source lines are zero at all points outside of the respective Mach cones. The expressions for the u-integrand in equation (1) are therefore evaluated along the section for values of x beginning at the forward boundary of the Mach cone. This integration gives the section-drag-coefficient components. In order to obtain the wing wave-drag coefficient, the section-wave-drag-coefficient components obtained from the respective u-expressions are evaluated along the wing span for values of y contained within the Mach cone. Table I refers to one side of the wing (x and y positive) and shows the limits of integration for x and y for the required u-expressions for the wings with sweptback and rectangular plan forms (fig. 2).

APPENDIX B

FORMULAS FOR WAVE-DRAG COEFFICIENTS FOR UNTAPERED SWEPTBACK AND RECTANGULAR WINGS OF BICONVEX PARABOLIC-ARC PROFILE AT ZERO LIFT $\left[m = \cot \Lambda \geq \frac{1}{\beta}\right]$

In the following analysis the quantities y and K are employed nondimensionally in terms of the semichord. The equations for the drag coefficients in all cases refer to the real parts of the indicated expressions.

Section Wave-Drag Coefficients for Sweptback Wings

Section wave-drag coefficient without tip effects.- The section drag coefficient obtained from equation (1) for the given wing at a spanwise station y and Mach number M without the tip effect was found to be as follows:

$$c_{d_\infty}(y) = \frac{8}{\pi}\left(\frac{t}{c}\right)^2 m \left\{ K^3 \cosh^{-1}\frac{K+2}{Km'} + \frac{1}{3\sqrt{m'^2-1}}\left[2\cos^{-1}\frac{2-K(m'^2-1)}{2m'} - 2(2K^3-3K-1)\cos^{-1}\frac{K(1+m'^2)+2}{2m'(K+1)}\right] - \frac{K^2}{3}\sqrt{(K+2)^2-(Km')^2}\right\} \tag{B1}$$

where $K = \frac{y}{m}$ and $m' = m\beta$. At the center section, where y or $K = 0$, equation (B1) becomes:

$$c_{d_\infty} = \frac{32}{3\pi}\left(\frac{t}{c}\right)^2 \frac{m}{\sqrt{m^2\beta^2-1}} \cos^{-1}\frac{1}{m\beta}$$

When $K = \frac{2}{m\beta - 1}$ or $y = \frac{2m}{m\beta - 1}$, the forward Mach line from the center section intersects the wing trailing edge, and for $y \geqq \frac{2m}{m\beta - 1}$ equation (B1) reduces to the following expression:

$$c_{d_\infty} = \frac{16}{3}\left(\frac{t}{c}\right)^2 \frac{m}{\sqrt{m^2\beta^2 - 1}}$$

Increment in section wave-drag coefficient caused by wing tips.— The increment in c_d caused by the tips depends on the sweep angle, aspect ratio, and Mach number. The following types occur in an untapered wing:

I. If $A \geqq \frac{2m}{m\beta + 1}$, each tip affects solely its own half of the wing. In this case the region of the wing affected is between values of y from $h - \frac{2m}{m\beta + 1}$ to h. (See fig. 2.) The increment in section wave-drag coefficient at a Mach number M and spanwise position y caused by the tip was found to be as follows:

$$\Delta c_{d_I}(y) = \frac{8}{\pi}\left(\frac{t}{c}\right)^2 m\left\{\frac{y_a'}{12m'^2}\left[\left(\frac{y_a'^2(m'^2 + 2)}{m'} - 12m'\right)\cosh^{-1}\frac{y_a' + 2m'}{|m'y_a'|} + \frac{(2m' - 3y_a')}{m'}\sqrt{4m'(y_a' + m') - y_a'^2(m'^2 - 1)}\right] - \frac{2}{3\sqrt{m'^2 - 1}}\cos^{-1}\frac{2m' - (m'^2 - 1)y_a'}{2m'^2}\right\} \qquad (B2)$$

where the subscript a indicates that the x-axis is shifted to the tip section, and where $y_a' = y_a\beta$ and $m' = m\beta$. In the plan form of the wing

$$y = y_a + h$$

In equation (B2) values for y_a are taken from $-\frac{2m}{m\beta + 1}$ to 0.

II. If $A < \frac{2m}{m\beta + 1}$, the tip on the opposite wing panel contributes an increment in c_d in addition to that discussed

under type I. (See fig. 2.) The increment in Δc_d at a section caused by the opposite tip was obtained in the following form:

$$\Delta c_{d_{II}}(y) = \frac{8}{\pi}\left(\frac{t}{c}\right)^2 m\left(\frac{y_b'}{m'^3}\left\{\frac{1}{12}\left(7y_b' - 10h' - 2m'\right)\sqrt{\left[y_b' - 2(h' - m')\right]^2 - (m'y_b')^2}\right.\right.$$
$$\left. - \left[\frac{y_b'^2}{12}\left(14 + m'^2\right) - 3h'y_b' + 2h'^2 - m'^2\right]\left[\cosh^{-1}\frac{y_b' - 2(h' - m')}{m'y_b'}\right]\right\}$$
$$+ \frac{2}{3m'^3\sqrt{m'^2 - 1}}\left[2y_b'^3 - 6y_b'^2h' + 3y_b'\left(2h'^2 - m'^2\right) - 2h'^3\right.$$
$$\left.\left. + 3m'^2h' - m'^3\right]\left[\cos^{-1}\frac{y_b'\left(1 + m'^2\right) - 2(h' - m')}{2m'\left(y_b' - h' + m'\right)}\right]\right) \qquad (B3)$$

where the subscript b indicates that the x-axis is shifted to the opposite tip section, and where $y_b' = y_b\beta$, $m' = m\beta$, and $h' = h\beta$. In the plan form of the wing

$$y = y_b - h$$

The limits for y_b to be used in equation (B3) depend on the value of the aspect ratio A. Thus

(a) If $A < \frac{2m}{m\beta + 1} > 1$, the front Mach line from the opposite tip intersects the trailing edge at a value of $y_b = \frac{2(m - h)}{m\beta - 1}$, so that values for y_b in equation (B3) are taken from h to $\frac{2(m - h)}{m\beta - 1}$.

(b) If $A < \frac{2m}{m\beta + 1} < 1$, the front Mach line from the opposite tip intersects the tip section, and values for y_b in equation (B3) are taken from h to $2h$.

In cases (a) and (b) discussed under type II, the increment in Δc_d caused by the adjacent tip discussed under type I is obtained at spanwise positions of y_a from $-h$ to 0.

The total increment in wave-drag coefficient at a section caused by the tips is given by

$$\Delta c_d = \Delta c_{d_I} + \Delta c_{d_{II}}$$

and the total wave-drag coefficient at the section is

$$c_d = c_{d_\infty} + \Delta c_d$$

Section Wave-Drag Coefficients for Rectangular Wings

For the rectangular wing, $m' = m\beta = \infty$ and the following equations result from equations (B1) to (B3):

Section wave-drag coefficient without tip effect.- For all values of y

$$c_{d_\infty} = \frac{16}{3\beta}\left(\frac{t}{c}\right)^2 \tag{B4}$$

This result agrees with Ackeret's theory for the biconvex parabolic-arc profile.

Increment in section wave-drag coefficient caused by wing tips.- If $A \geq \frac{2}{\beta}$, the tip effect results solely from the adjacent tip and

$$\Delta c_{d_I} = \frac{8}{3\pi\beta}\left(\frac{t}{c}\right)^2 \left\{ \frac{y_a'}{4}\left[\left(y_a'^2 - 12\right)\cosh^{-1}\frac{2}{|y_a'|} + 2\sqrt{4 - y_a'^2}\right] - 2\cos^{-1}\frac{y_a'}{2} \right\} \tag{B5}$$

where

$$y_a' = y_a\beta = (y - h)\beta$$

In equation (B5), values for y_a are taken from $-\frac{2}{\beta}$ to 0.

If $A < \frac{2}{\beta}$, the tip on the opposite wing panel contributes an increment in c_d in addition to Δc_{d_I}. The increment in Δc_d at a section caused by the opposite tip is

$$\Delta c_{d_{II}} = \frac{8}{3\pi\beta}\left(\frac{t}{c}\right)^2\left\{-\frac{y_b'}{4}\left[\left(y_b'^2 - 12\right)\cosh^{-1}\frac{2}{y_b'} + 2\sqrt{4 - y_b'^2}\right] - 2\cos^{-1}\frac{y_b'}{2}\right\} \tag{B6}$$

where

$$y_b' = y_b\beta = (y + h)\beta$$

The values for y_b' or y which are required in equation (B6) for $A < \frac{2}{\beta}$ are as follows (see fig. 2(b)):

(a) If $A > \frac{1}{\beta}$, y varies from 0 to $\frac{2}{\beta} - h$

(b) If $A < \frac{1}{\beta}$, y varies from 0 to h

Wing Wave-Drag Coefficients for Sweptback Wings

The integrations of equations (B1) to (B3) for the section wave-drag coefficients between the appropriate limits for y (fig. 2(a) and table I) yield the following results for the sweptback wing.

Wing wave-drag coefficient without tip effect.- The wing wave-drag coefficient without tip effect is

$$C_{D_\infty} = \frac{8}{\pi}\left(\frac{t}{c}\right)^2 m\left\{\frac{A'^2}{12m'^3}\left[3A' \cosh^{-1}\frac{A' + 2m'}{A'm'} - \sqrt{4m'(A' + m') - A'^2(m'^2 - 1)}\right]\right.$$

$$+ \frac{1}{3m'^3\sqrt{m'^2 - 1}}\left[2m'^3 \cos^{-1}\frac{2m' - A'(m'^2 - 1)}{2m'^2}\right.$$

$$\left.\left. + \left(2m'^3 + 3A'm'^2 - A'^3\right) \cos^{-1}\frac{2m' + A'(m'^2 + 1)}{2m'(A' + m')}\right]\right\} \qquad (B7)$$

where $A' = A\beta$ and $m' = m\beta$.

Increment in wing wave-drag coefficient caused by tips.- If $A \geq \frac{2m}{m\beta + 1}$, the contribution of the tips to the wing wave-drag coefficient is zero.

If $A < \frac{2m}{m\beta + 1} > \frac{1}{\beta}$, then

$$\Delta C_D = \frac{8}{\pi}\left(\frac{t}{c}\right)^2 m\left\{\frac{1}{3\sqrt{m'^2 - 1}}\left[-2 \cos^{-1}\frac{A'(m'^2 - 1) + 2m'}{2m'^2}\right.\right.$$

$$\left. + \frac{(2m'^3 - 3m'^2A' + A'^3)}{m'^3} \cos^{-1}\frac{A'(m'^2 + 1) - 2m'}{2m'(m' - A')}\right]$$

$$\left. + \frac{A'^2}{12m'^3}\left[3A' \cosh^{-1}\frac{2m' - A'}{m'A'} + \sqrt{4m'(m' - A') - A'^2(m'^2 - 1)}\right]\right\} \qquad (B8)$$

If $A < \frac{1}{\beta}$, then

$$\Delta C_D = \frac{8}{\pi}\left(\frac{t}{c}\right)^2 m \left(\frac{1}{3m'^3\sqrt{m'^2-1}} \left[-2m'^3 \cos^{-1}\frac{A'(m'^2-1)+2m'}{2m'^2} \right.\right.$$

$$+ (2m'^3 - 3m'^2A' + A'^3)\cos^{-1}\frac{A'(m'^2+1)-2m'}{2m'(m'-A')}$$

$$+ (A' - 2m')(m' + A')^2 \cos^{-1}\frac{m'A'+1}{m'+A'}$$

$$\left. - (A' + 2m')(m' - A')^2 \cos^{-1}\frac{m'A'-1}{m'-A'} \right]$$

$$+ \frac{A'}{12m'^3}\left\{ 4\left[6m'^2 - A'^2\left(m'^2+2\right)\right]\cosh^{-1}\frac{1}{A'} - 4m'^2\sqrt{1-A'^2} \right.$$

$$\left. \left. + 3A'^2 \cosh^{-1}\frac{2m'-A'}{m'A'} + A'\sqrt{4m'(m'-A') - A'^2(m'^2-1)} \right\} \right) \qquad (B9)$$

Total wing wave-drag coefficient.- The total wing wave-drag coefficient is obtained as the sum,

$$C_D = C_{D_\infty} + \Delta C_D$$

where the components C_{D_∞} and ΔC_D are calculated from the foregoing equations for the wing wave-drag coefficient appropriate to the aspect ratio of the wing.

Wing Wave-Drag Coefficients for Rectangular Wings

For the rectangular wing, $m' = m\beta = \infty$. The following results for the wave-drag coefficient of the rectangular wing may be obtained either by integrations of equations (B4) to (B6) between the appropriate limits for y (see fig. 2(b)) or by substitution of $m = \infty$ in equations (B7) to (B9):

Wing wave-drag coefficient without tip effect.- The wing wave-drag coefficient without tip effect is

$$C_{D_\infty} = \frac{16}{3\beta}\left(\frac{t}{c}\right)^2 \qquad (B10)$$

This result agrees with Ackeret's theory for a biconvex parabolic-arc profile.

Increment in wing wave-drag coefficient caused by tips.- The increment in C_D contributed by the tips is obtained in the form

$$\Delta C_D = \frac{8}{\pi\beta}\left(\frac{t}{c}\right)^2 \left\{ -\frac{4}{3}\cos^{-1} A' + \frac{A'}{3}\left[\left(6 - A'^2\right)\cosh^{-1}\frac{1}{A'} - \sqrt{1 - A'^2}\right]\right\} \qquad \text{(B11)}$$

where

$$A' = A\beta < 1$$

If $A \geq \frac{1}{\beta}$, equation (B11) shows that $\Delta C_D = 0$.

REFERENCES

1. Puckett, Allen E.: Supersonic Wave Drag of Thin Airfoils. Jour. Aero. Sci., vol. 13, no. 9, Sept. 1946, pp. 475-484.

2. Jones, Robert T.: Thin Oblique Airfoils at Supersonic Speed. NACA TN No. 1107, 1946.

3. Harmon, Sidney M., and Swanson, Margaret D.: Calculations of the Supersonic Wave Drag of Nonlifting Wings with Arbitrary Sweepback and Aspect Ratio. Wings Swept behind the Mach Lines. NACA TN No. 1319, 1947.

4. Busemann, A.: Aerodynamic Lift at Supersonic Speeds. 2844, Ae. Techl. 1201, British A.R.C., Feb. 3, 1937. (From Luftfahrtforschung, Bd. 12, Nr. 6, Oct. 3, 1935, pp. 210-220.)

5. Taylor, G. I.: Applications to Aeronautics of Ackeret's Theory of Aerofoils Moving at Speeds Greater Than That of Sound. R. & M. No. 1467, British A.R.C., 1932.

TABLE I

LIMITS OF INTEGRATION FOR WINGS WITH SWEPTBACK AND RECTANGULAR PLAN FORMS

u-components	Limits of Integration			
	x		y	
	Lower limit	Upper limit	Lower limit	Upper limit
Sweptback wings				
$u_{0,0}$ $\bar{u}_{0,0}$ $\frac{1}{D}u_{0,0}$ $\frac{1}{D}\bar{u}_{0,0}$	y/m	$\frac{y}{m} + c$	0	h
$u_{h/m,h}$ $\frac{1}{D}u_{h/m,h}$	$\frac{h}{m}(m\beta + 1) - y\beta$	$\frac{y}{m} + c$	$h - \frac{mc}{m\beta + 1}$ $\left(\text{if } A > \frac{2m}{m\beta + 1}\right)$ 0 $\left(\text{if } A \leq \frac{2m}{m\beta + 1}\right)$	h
[a] $\bar{u}_{h/m,-h}$ $\frac{1}{D}\bar{u}_{h/m,-h}$	$\frac{h}{m}(m\beta + 1) + y\beta$	$\frac{y}{m} + c$	0	$\frac{mc - h(m\beta + 1)}{m\beta - 1}$ $\left(\text{if } \frac{2m}{m\beta + 1} > A > \frac{1}{\beta}\right)$ h $\left(\text{if } \frac{2m}{m\beta + 1} \geq A \leq \frac{1}{\beta}\right)$
Rectangular wings $(m = \infty)$				
$u_{0,0}$ $\bar{u}_{0,0}$ $\frac{1}{D}u_{0,0}$ $\frac{1}{D}\bar{u}_{0,0}$	0	c	0	h
$u_{0,h}$ $\frac{1}{D}u_{0,h}$	$\beta(h - y)$	c	$h - \frac{c}{\beta}$ $\left(\text{if } A > \frac{2}{\beta}\right)$ 0 $\left(\text{if } A \leq \frac{2}{\beta}\right)$	h
[b] $\bar{u}_{0,-h}$ $\frac{1}{D}\bar{u}_{0,-h}$	$\beta(h + y)$	$\frac{y}{m} + c$	0	$\frac{c}{\beta} - h$ $\left(\text{if } \frac{2}{\beta} > A > \frac{1}{\beta}\right)$ h $\left(\text{if } \frac{2}{\beta} \geq A \leq \frac{1}{\beta}\right)$

[a] The components $\bar{u}_{h/m,-h}$ and $\frac{1}{D}\bar{u}_{h/m,-h}$ are zero if $A \geq \frac{2m}{m\beta + 1}$; therefore, the integration limits for these u-components refer to cases in which $A < \frac{2m}{m\beta + 1}$.

[b] The components $\bar{u}_{0,-h}$ and $\frac{1}{D}\bar{u}_{0,-h}$ are zero if $A \geq \frac{2}{\beta}$; therefore, the integration limits for these u-components refer to cases in which $A < \frac{2}{\beta}$.

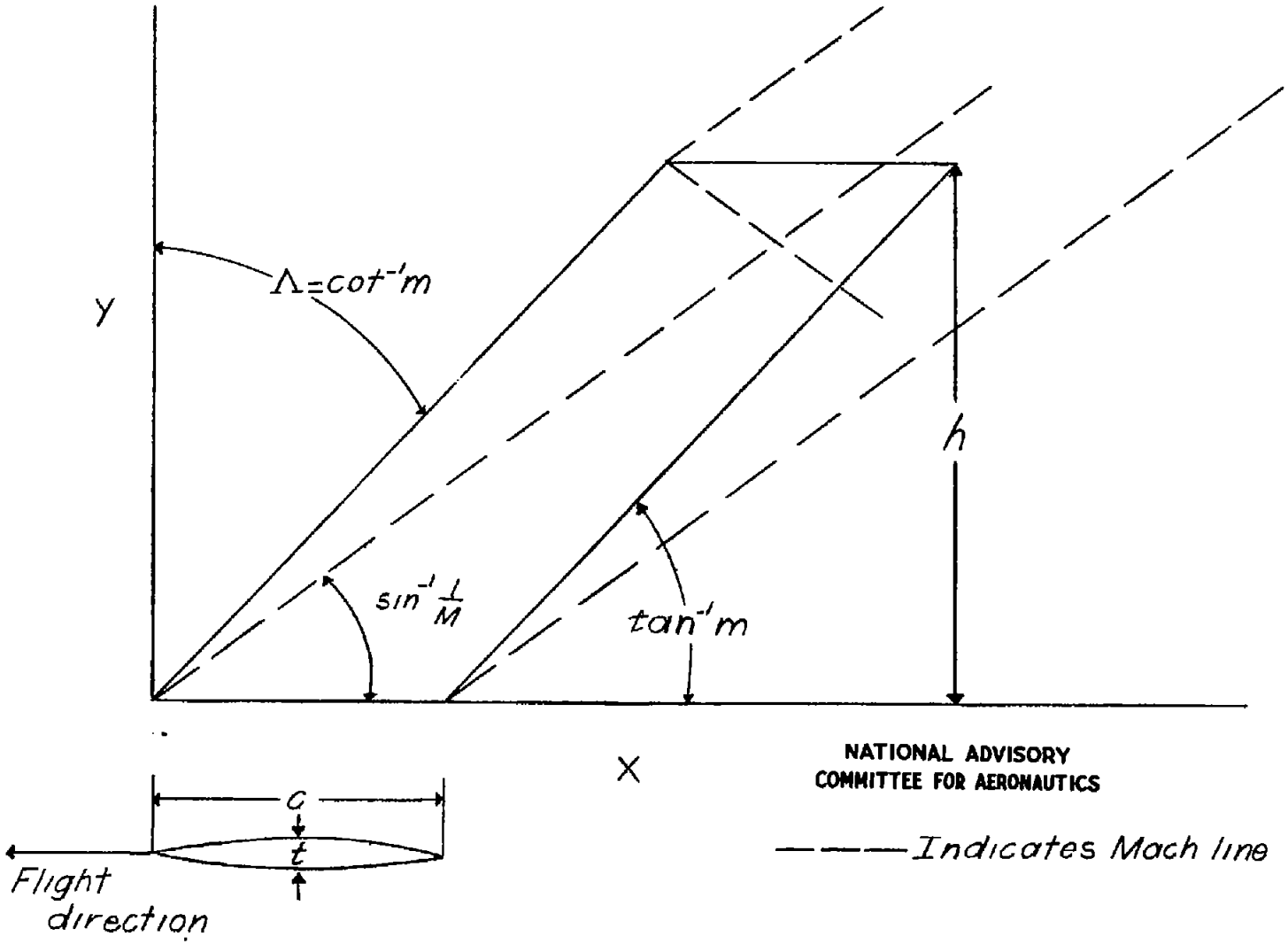

Figure 1.- Symbols for sweptback wings.

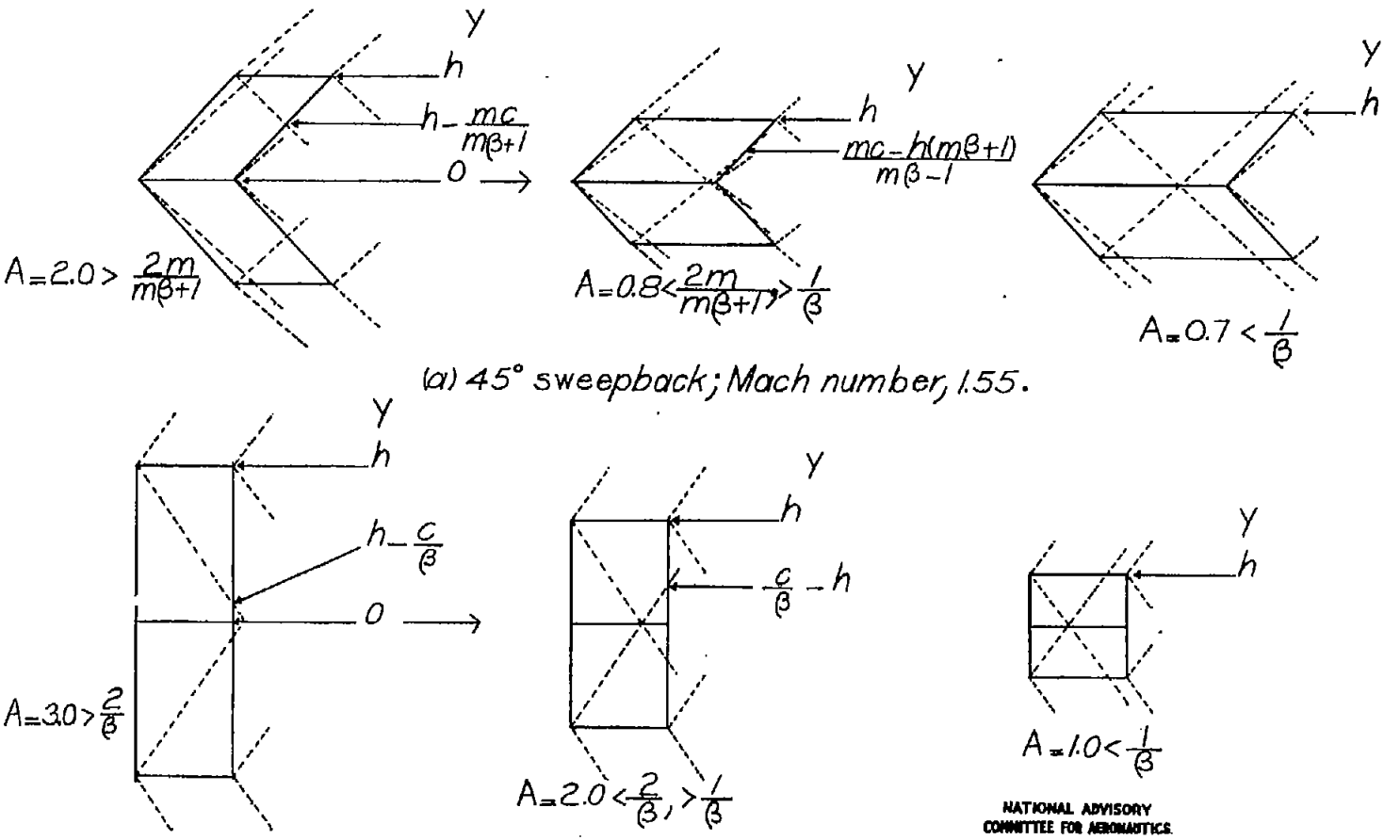

Figure 2.- Configurations showing typical Mach lines behind wing leading edge for various aspect ratios. Biconvex parabolic-arc profile; no taper.

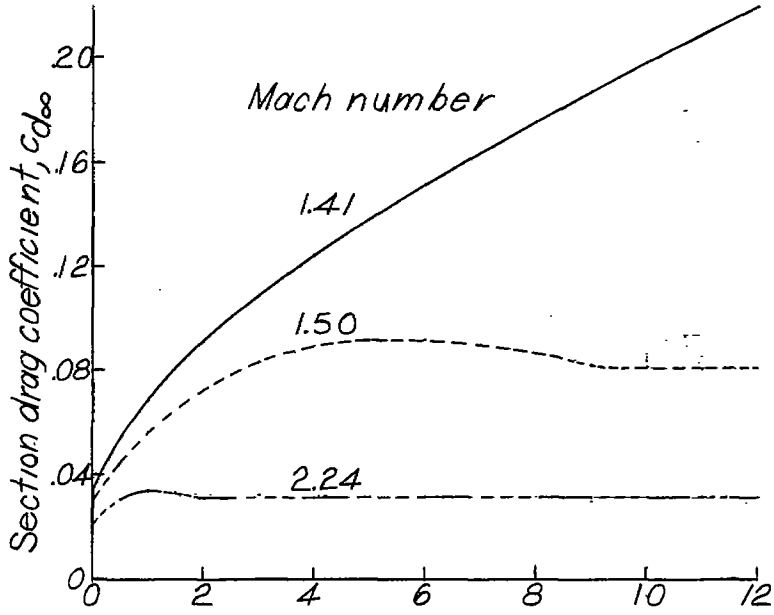

(a) Section-drag-coefficient distribution without tip effect for several Mach numbers.

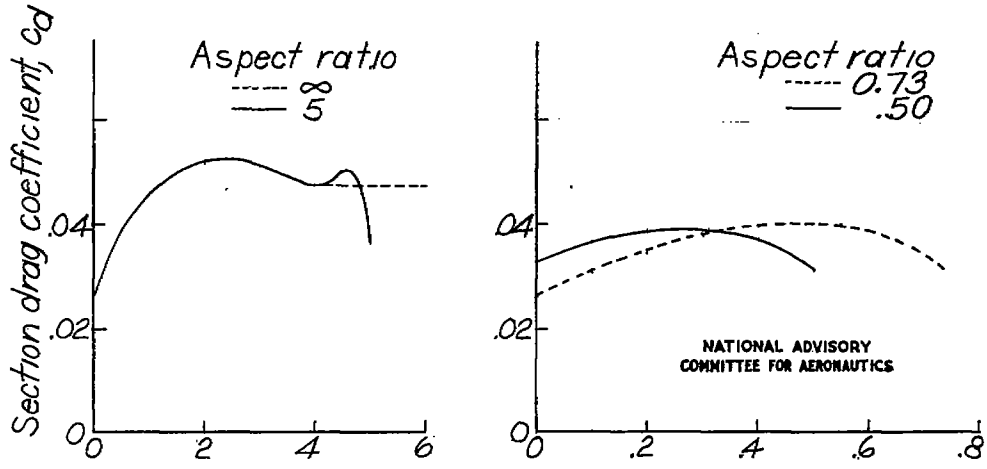

(b) Section-drag-coefficient distribution with tip effect; Mach number, 1.8.

Figure 3.- Typical distributions of section wave-drag coefficients along wing span for sweptback wing. Biconvex parabolic-arc profile at zero lift; no taper; $\frac{t}{c} = 0.10$; $\Lambda = 45^\circ$.

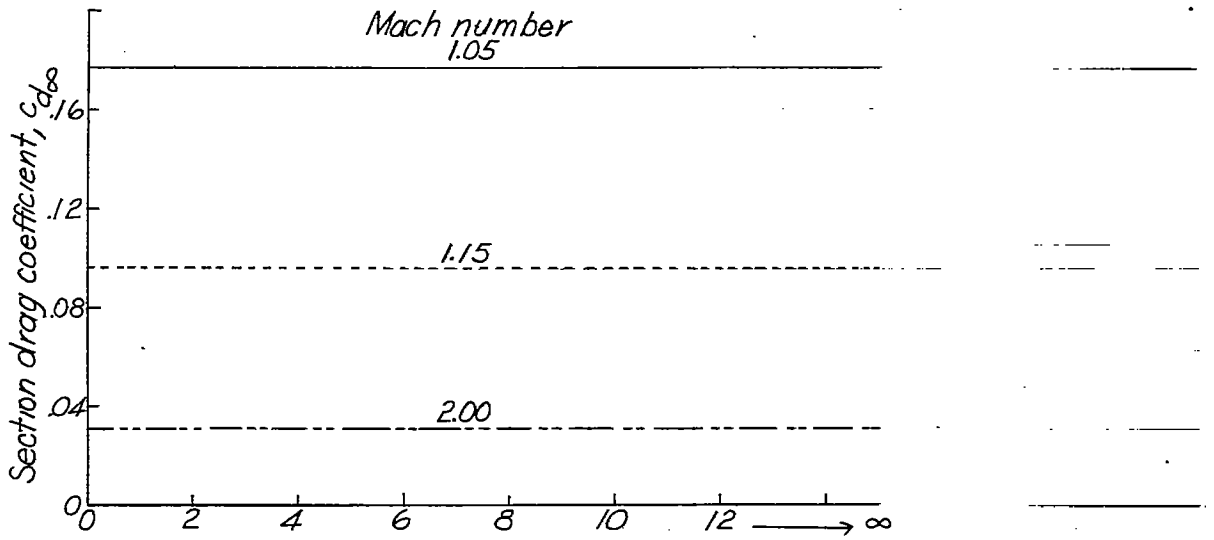

(a) Section-drag-coefficient distribution without tip effect for several Mach numbers.

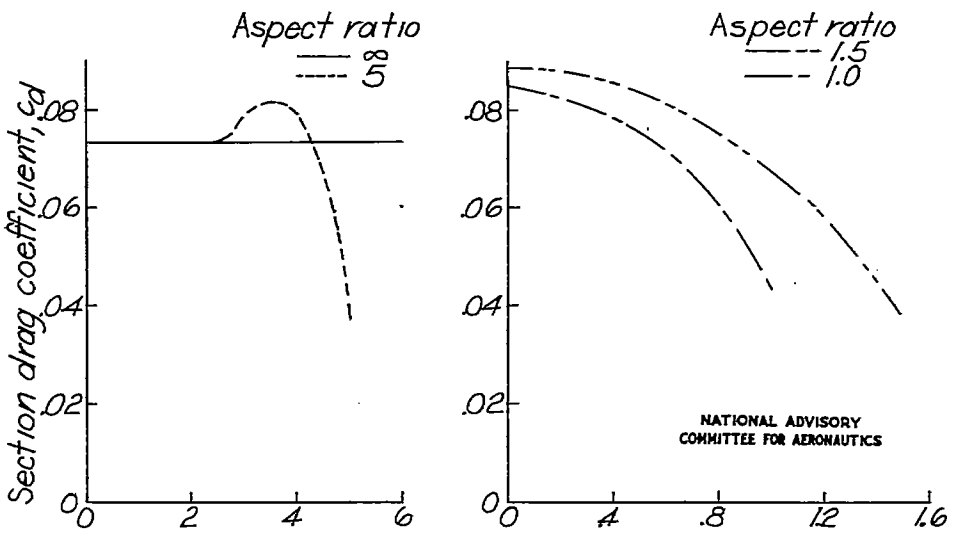

(b) Section-drag-coefficient distribution with tip effect; Mach number, 1.25.

Figure 4.- Typical distributions of section wave-drag coefficients along wing span for rectangular wing. Biconvex parabolic-arc profile at zero lift; $\frac{t}{c} = 0.10$; $\Lambda = 0^\circ$.

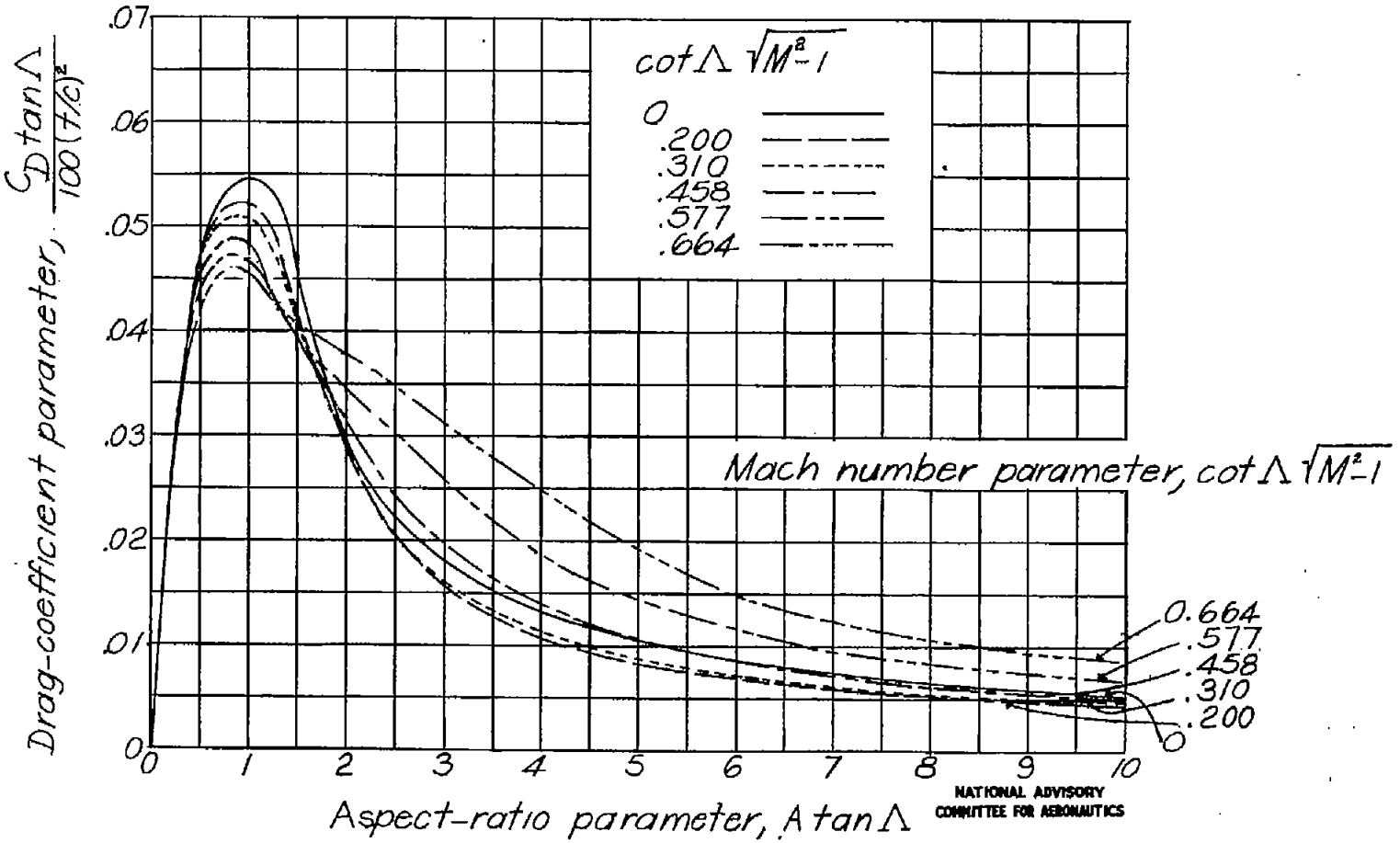

(a) $0 \leqq \cot\Lambda\sqrt{M^2 - 1} \leqq 0.664$.

Figure 5.- Generalized curves for determining variation of wing wave-drag coefficient with aspect ratio for constant sweepback angles, Mach numbers, and thickness ratios. Biconvex parabolic-arc profile at zero lift; no taper.

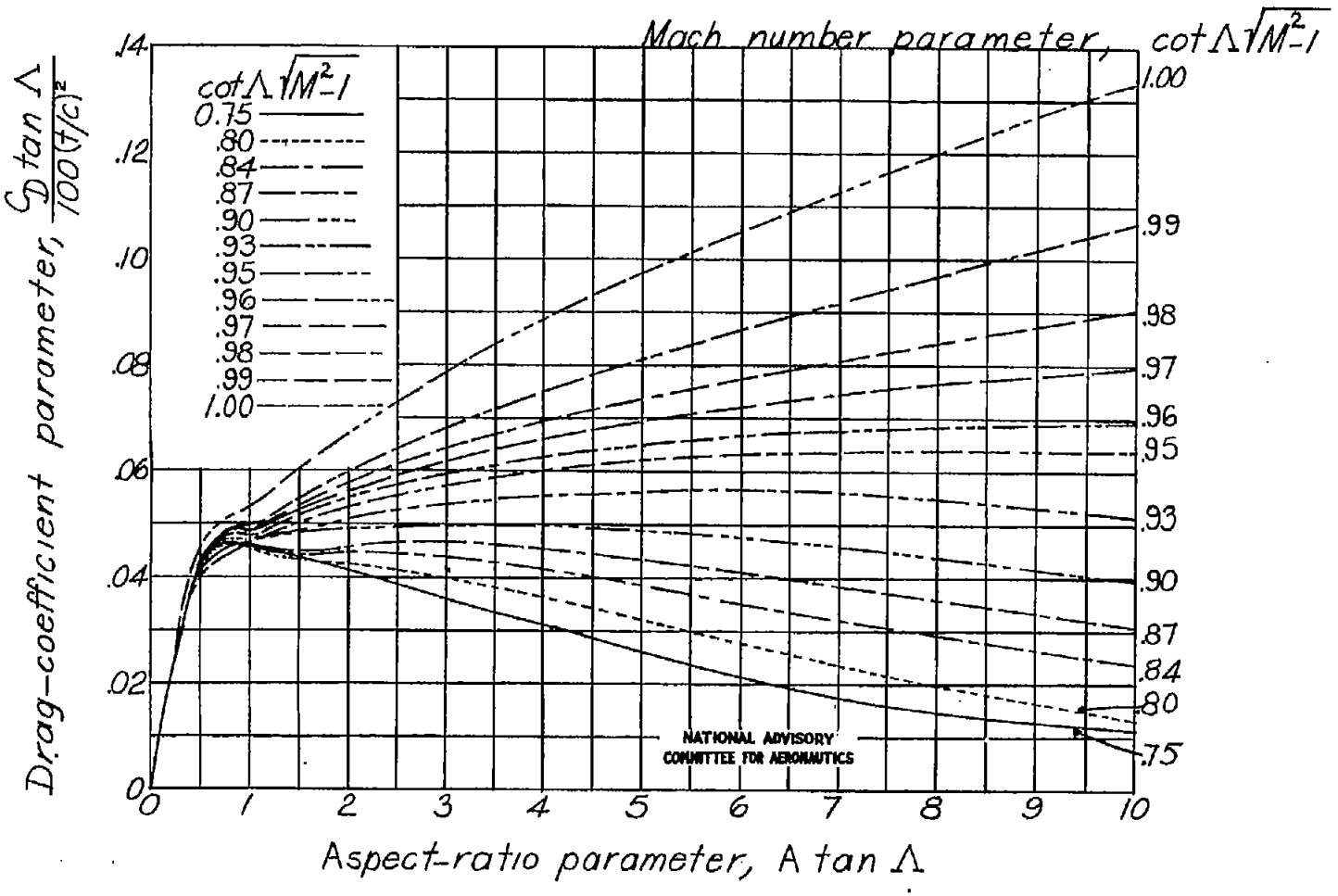

(b) $0.75 \leqq \cot \Lambda \sqrt{M^2 - 1} \leqq 1.00$.

Figure 5.- Continued.

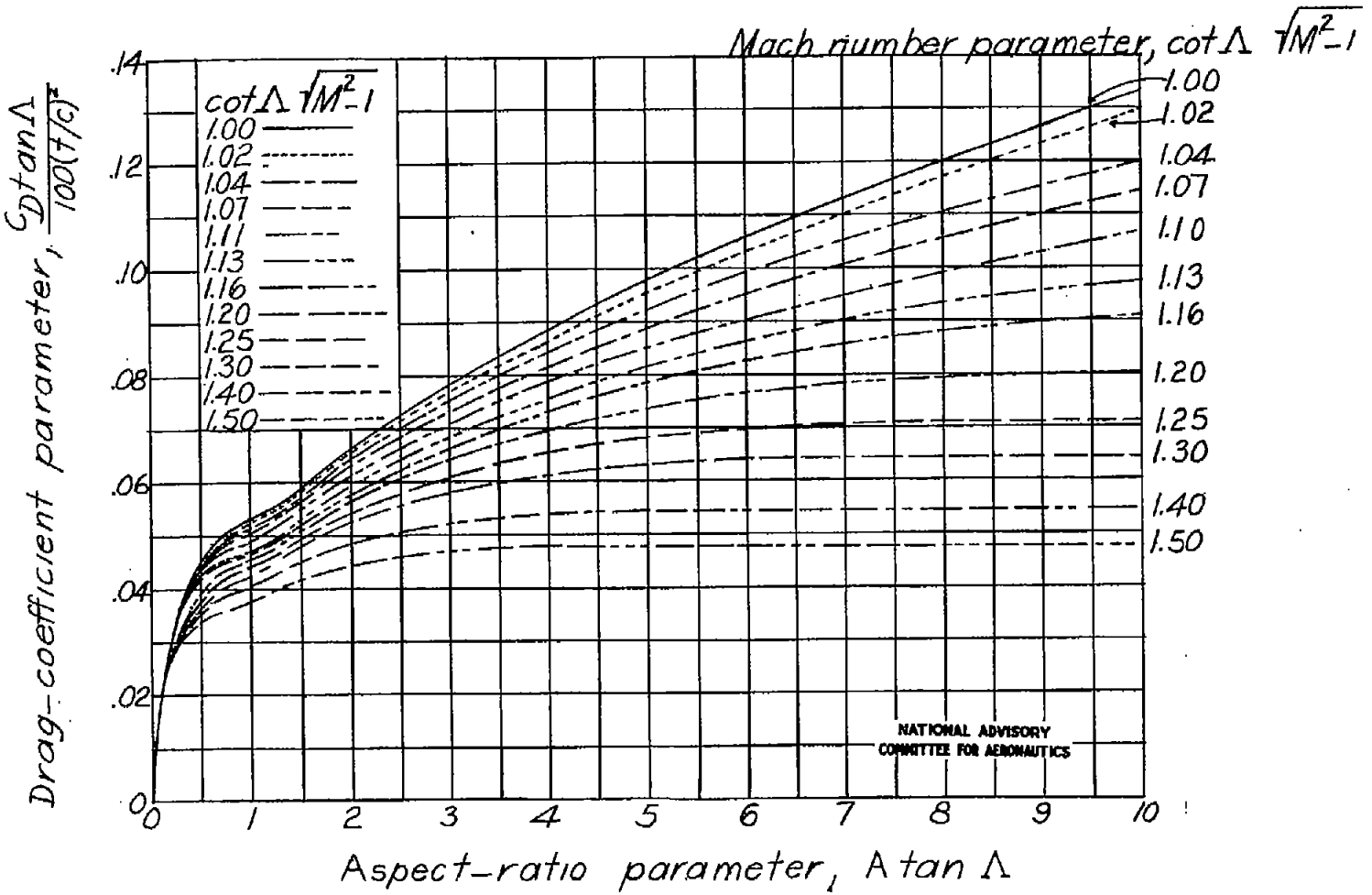

(c) $1.00 \leqq \cot \Lambda \sqrt{M^2 - 1} \leqq 1.50$.

Figure 5.- Continued.

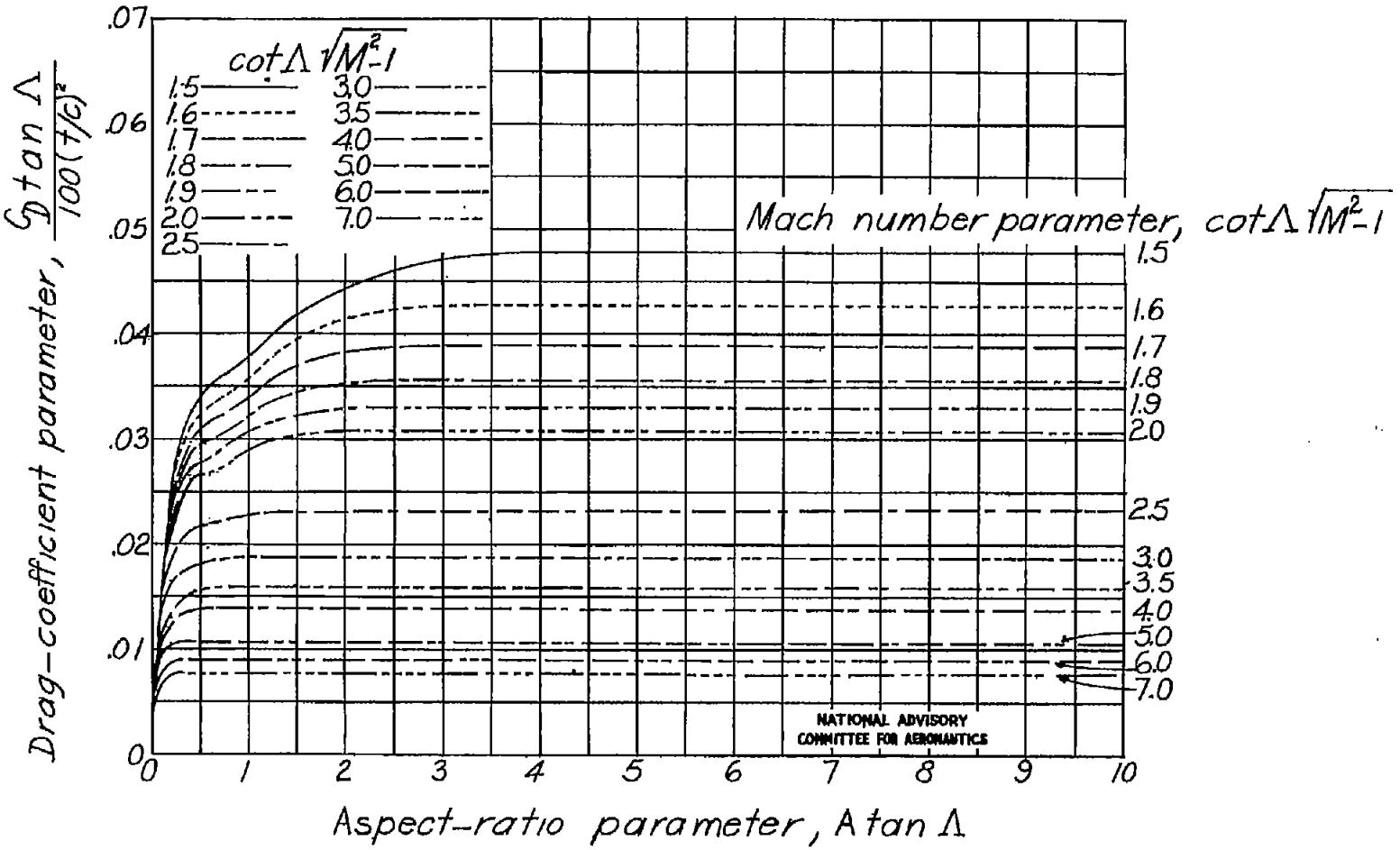

(d) $1.5 \leqq \cot \Lambda \sqrt{M^2 - 1} \leqq 7.0$

Figure 5.- Concluded.

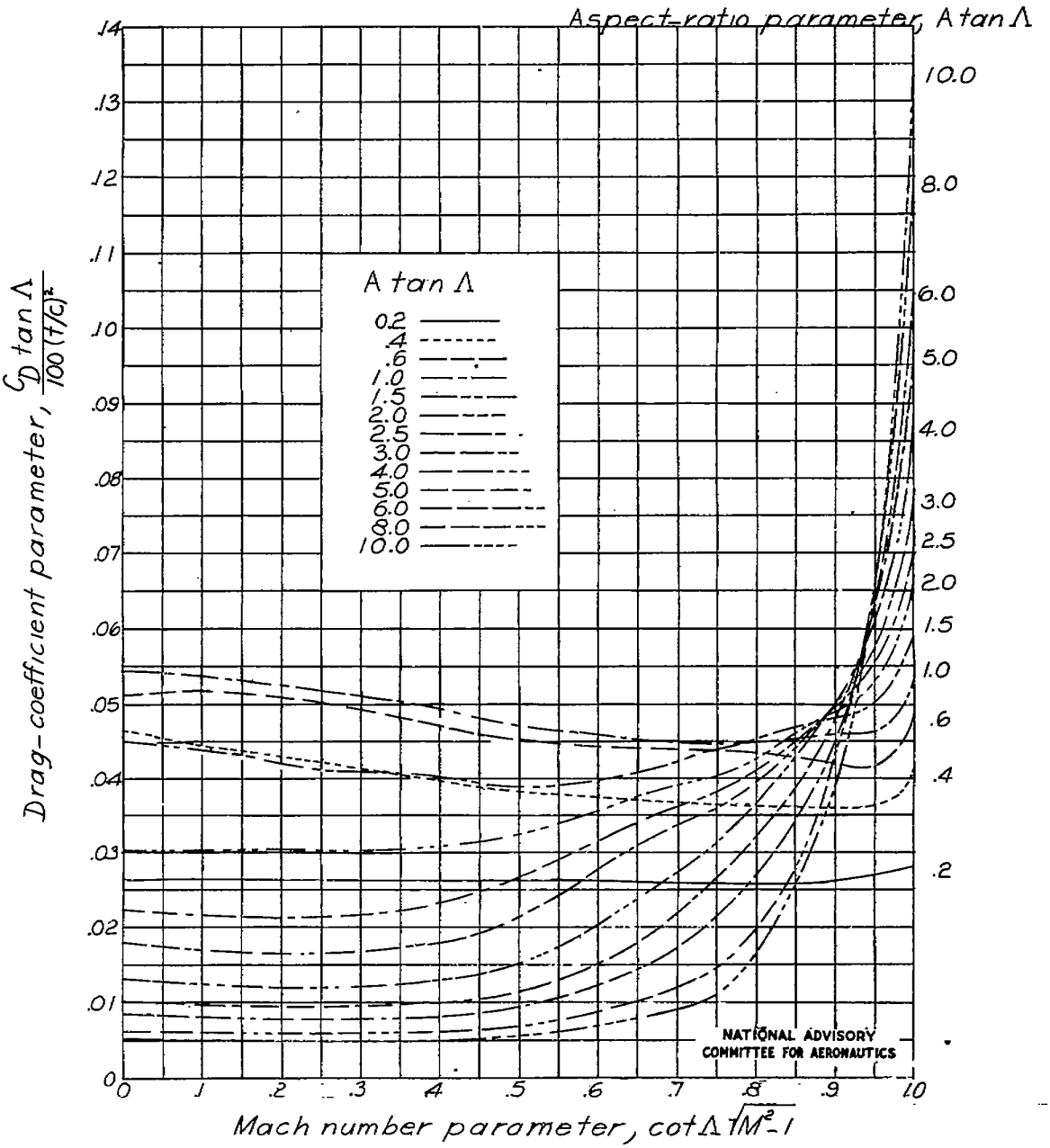

Figure 6.- Generalized curves for determining variation of wing wave-drag coefficient with Mach number for constant aspect ratios, sweepback angles, and thickness ratios. Biconvex parabolic-arc profile at zero lift; no taper.

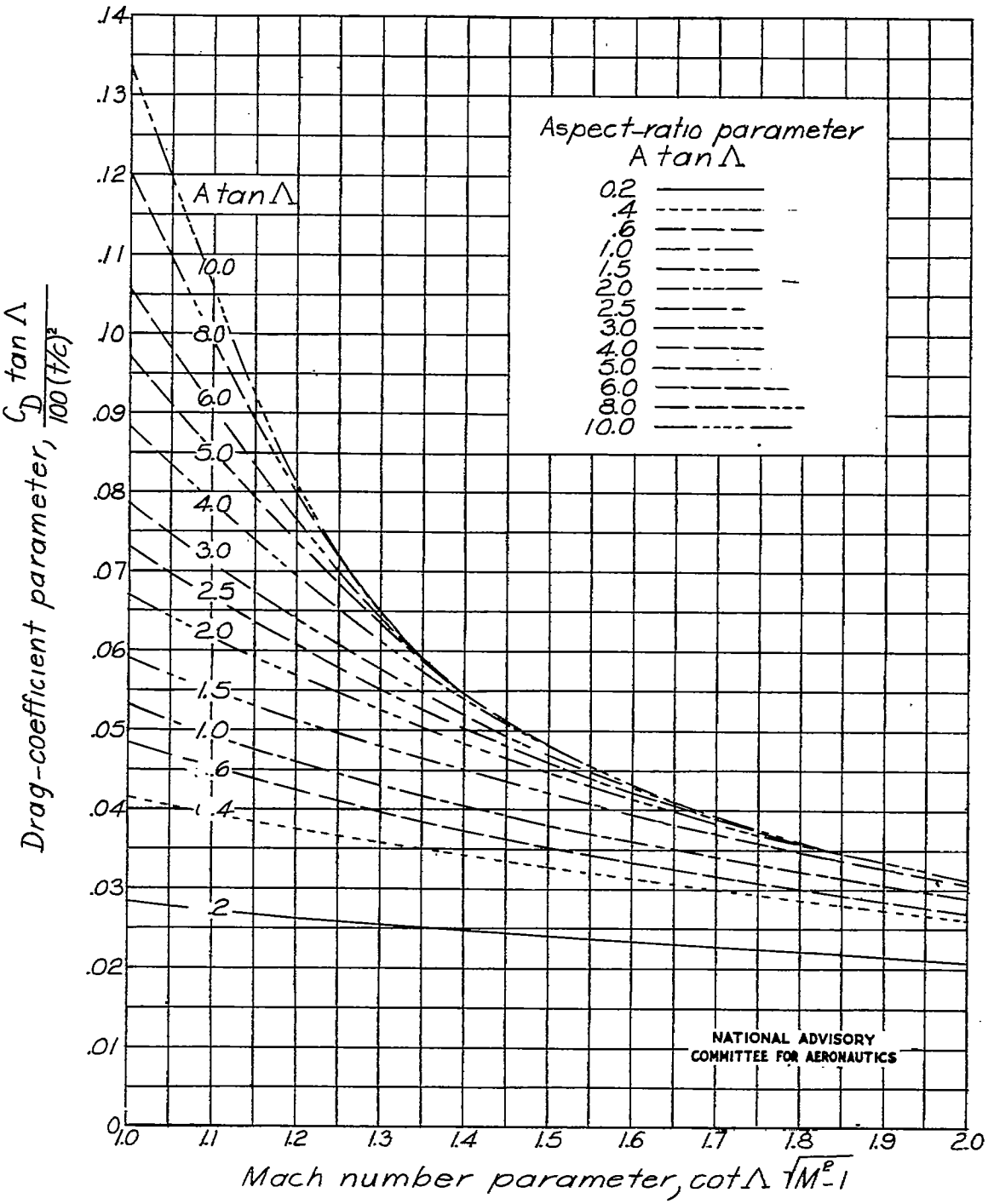

Figure 6.- Continued.

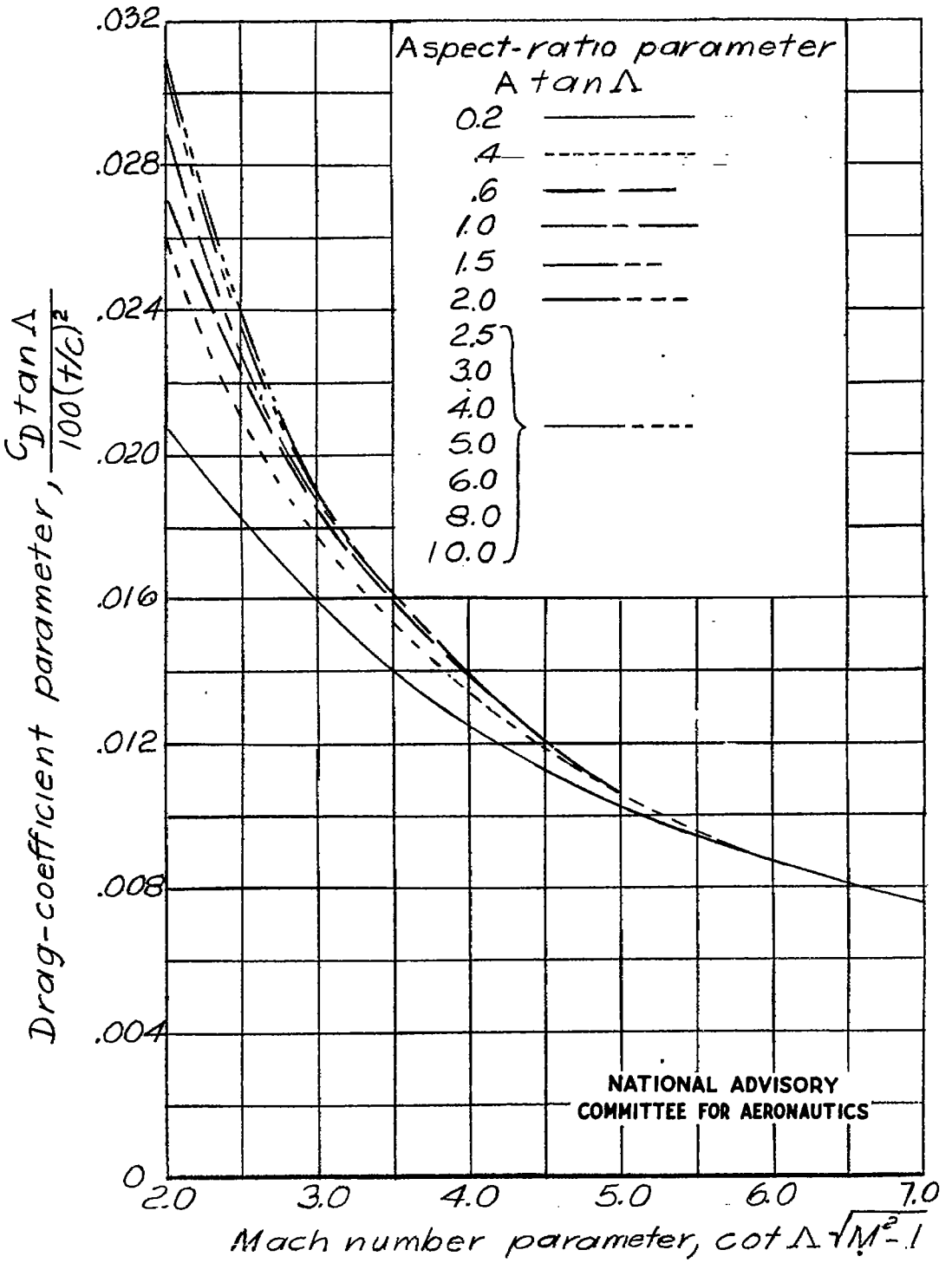

Figure 6.- Concluded.

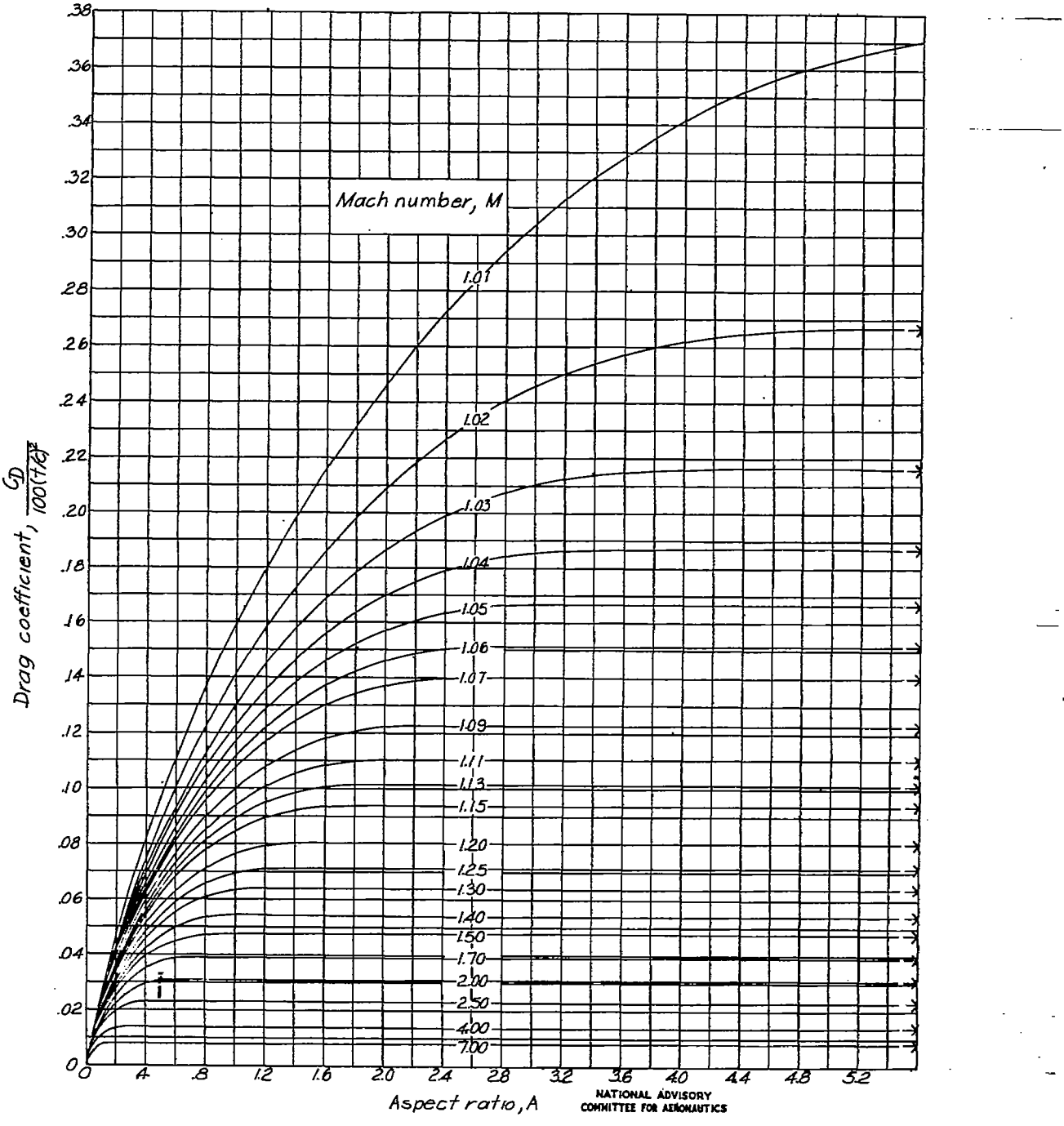

Figure 7.- Generalized curves for determining variation of wing wave-drag coefficient with aspect ratio for constant Mach numbers and thickness ratios for rectangular wing. Biconvex parabolic-arc profile at zero lift.

(Arrows indicate that values for $\frac{C_D}{100\,(t/c)^2}$ remain constant for all aspect ratios to infinity.)

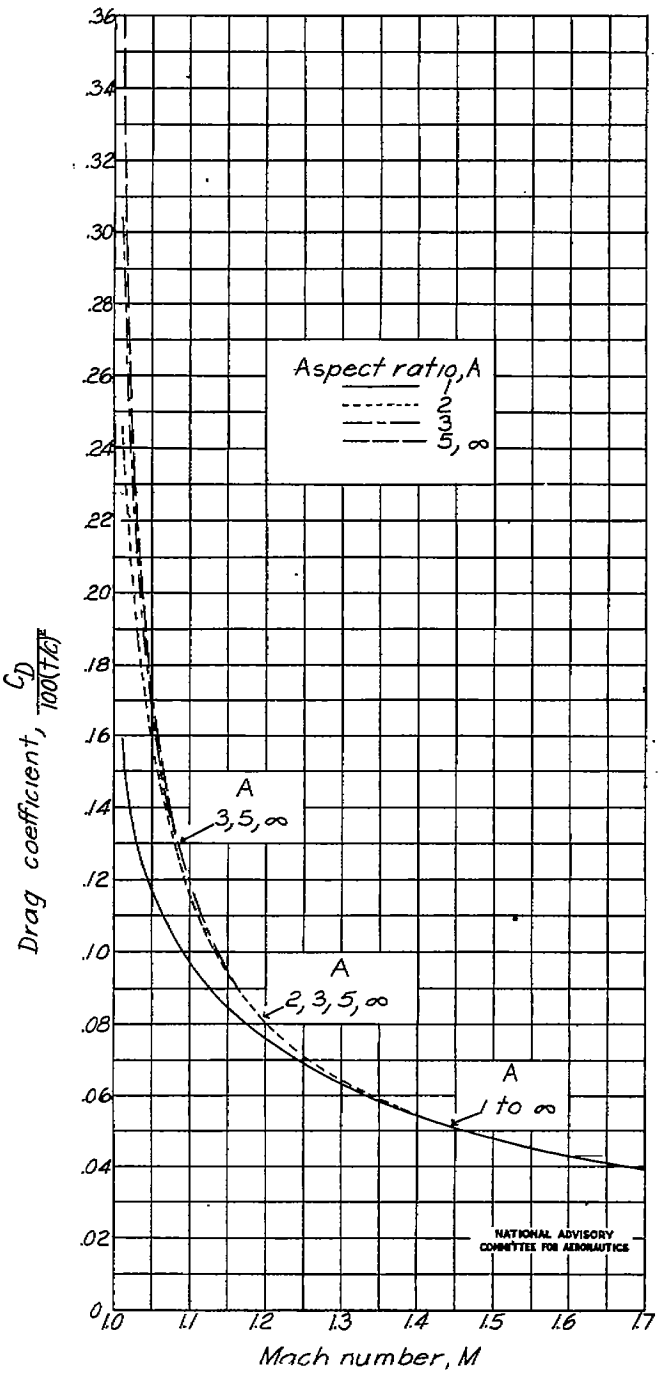

Figure 8.- Generalized curves for determining variation of wing wave-drag coefficient with Mach number for constant aspect ratios and thickness ratios for rectangular wing. Biconvex parabolic-arc profile at zero lift.

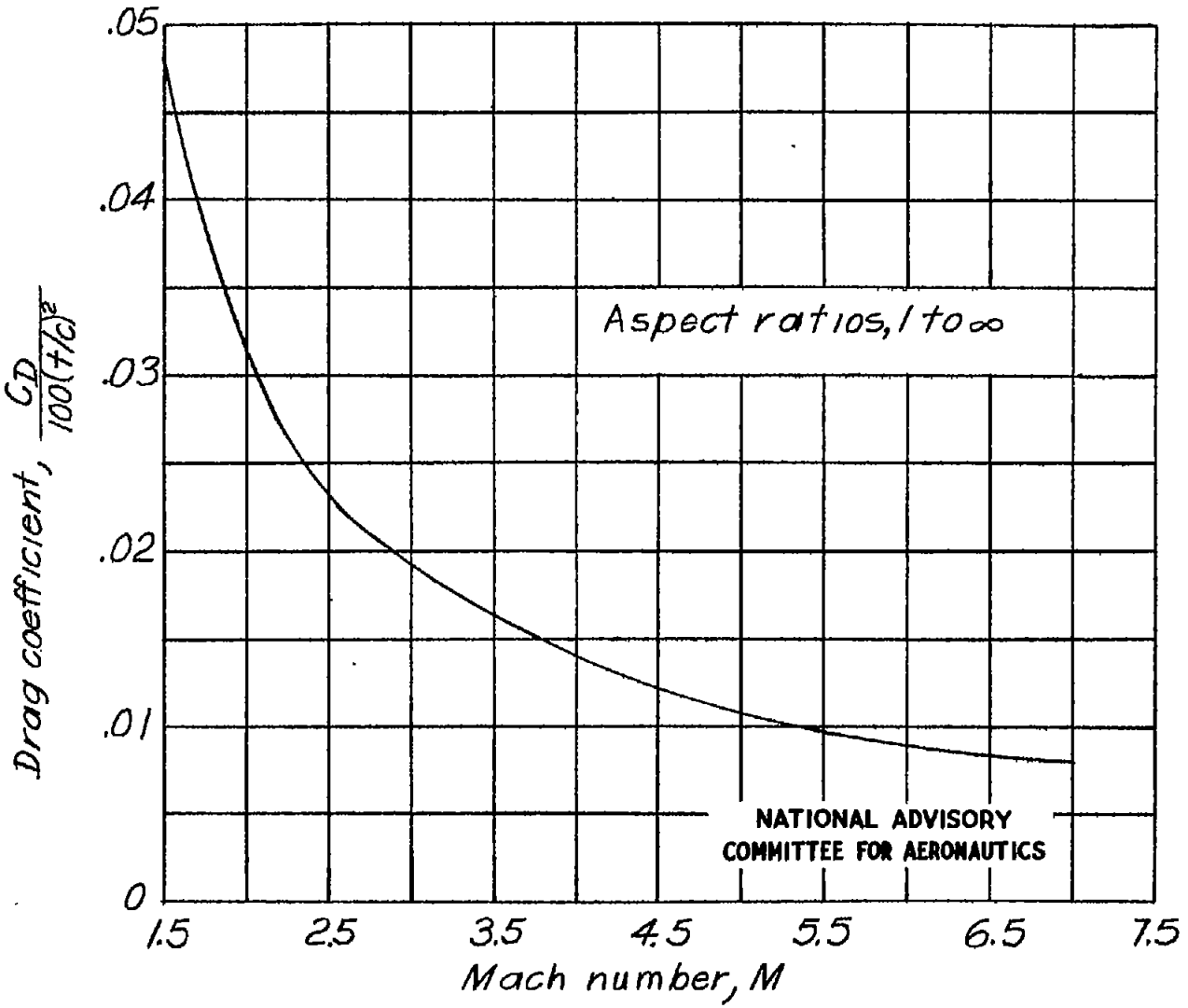

Figure 8.- Concluded.

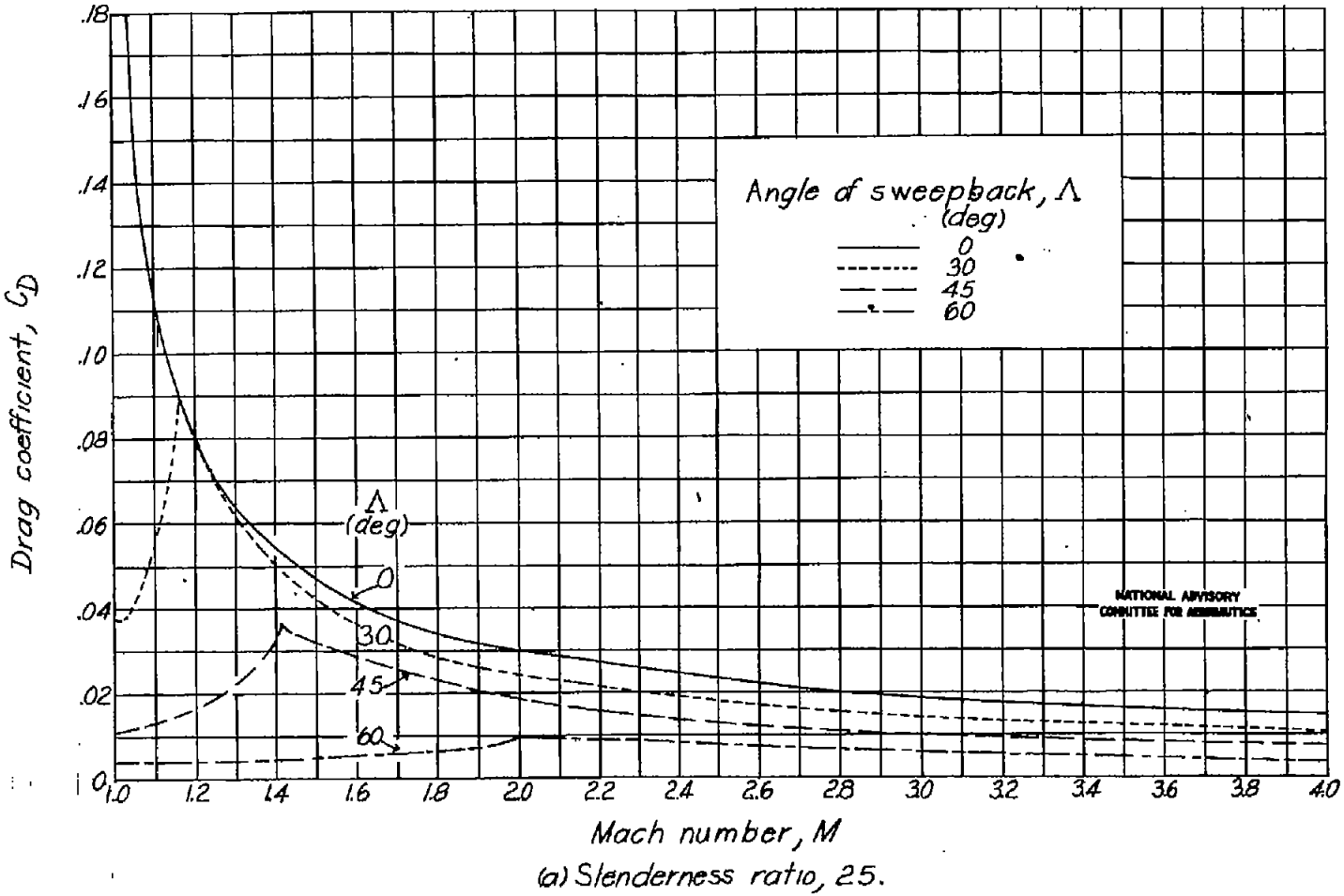

(a) Slenderness ratio, 25.

Figure 9.- Variation of wing wave-drag coefficient with Mach number for different sweepback angles with constant slenderness ratios. Biconvex parabolic-arc profile at zero lift; no taper; $A = 0.20 \frac{l}{t} \cos^2 \Lambda$; $\frac{t}{c} = 0.10 \cos \Lambda$; constant wing area.

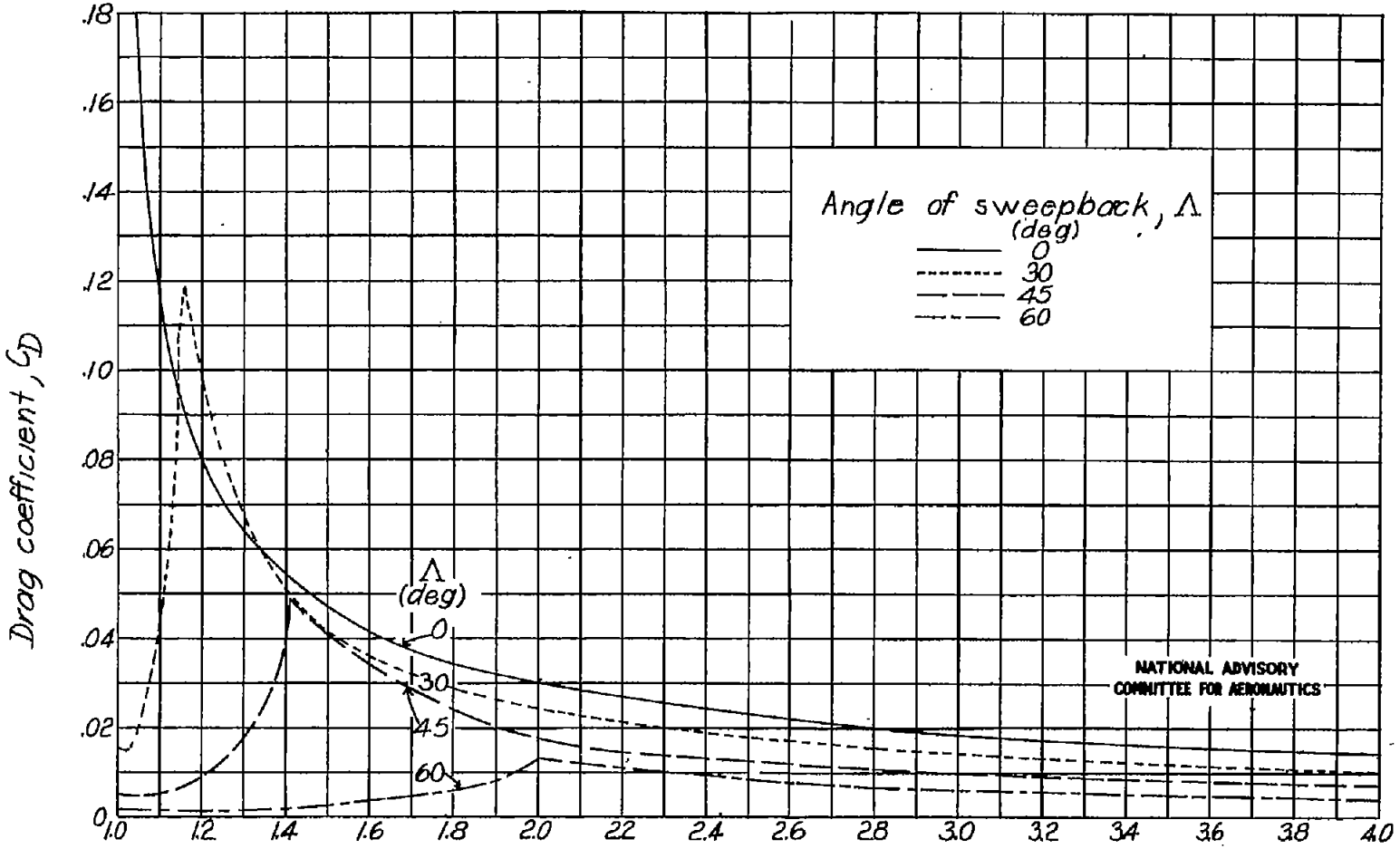

(b) Slenderness ratio, 50.

Figure 9.- Concluded.

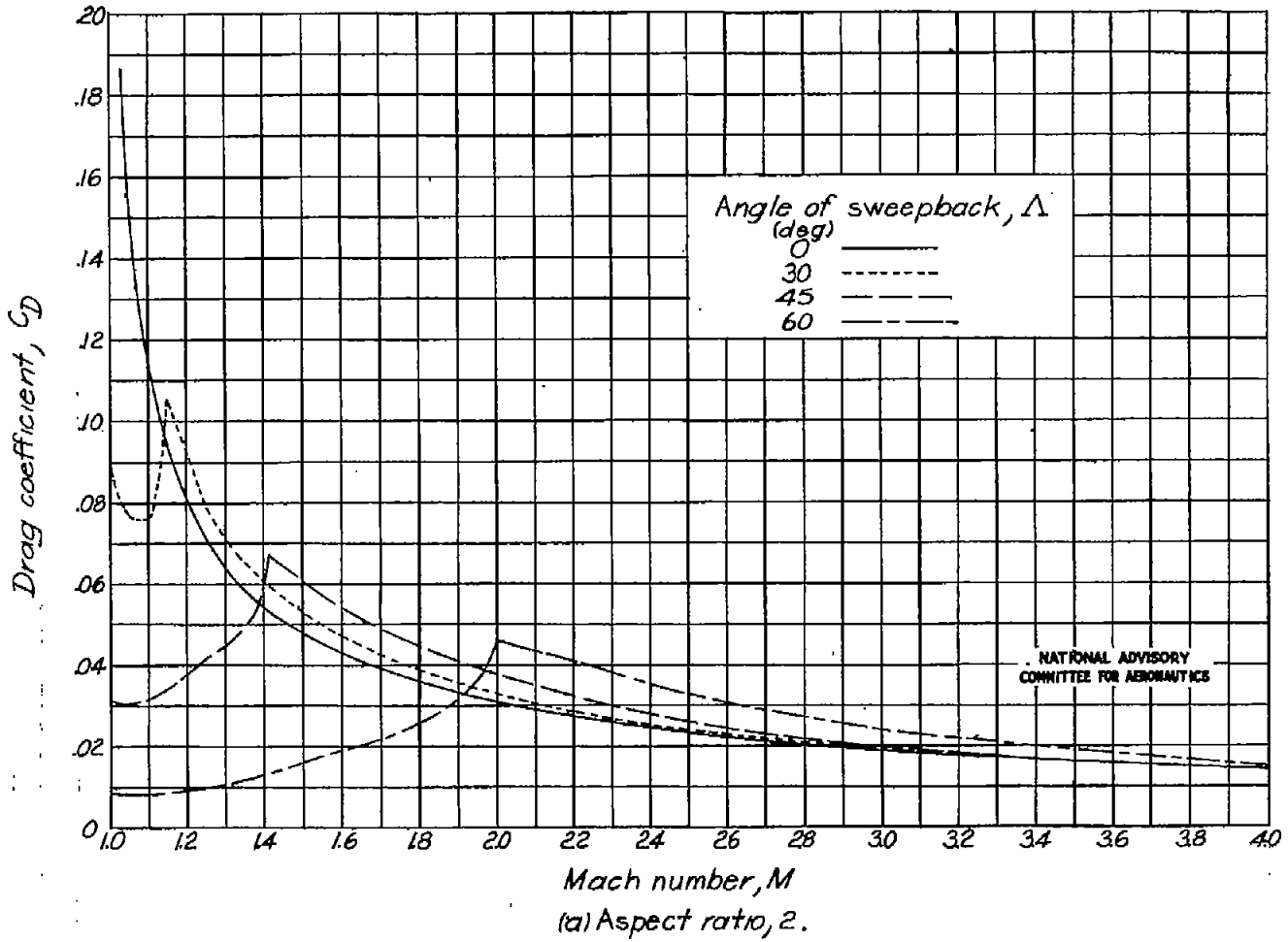

Figure 10.- Variation of wing wave-drag coefficient with Mach number for different sweepback angles with constant aspect ratios. Biconvex parabolic-arc profile at zero lift; no taper; $\frac{t}{c} = 0.10$; constant wing area.

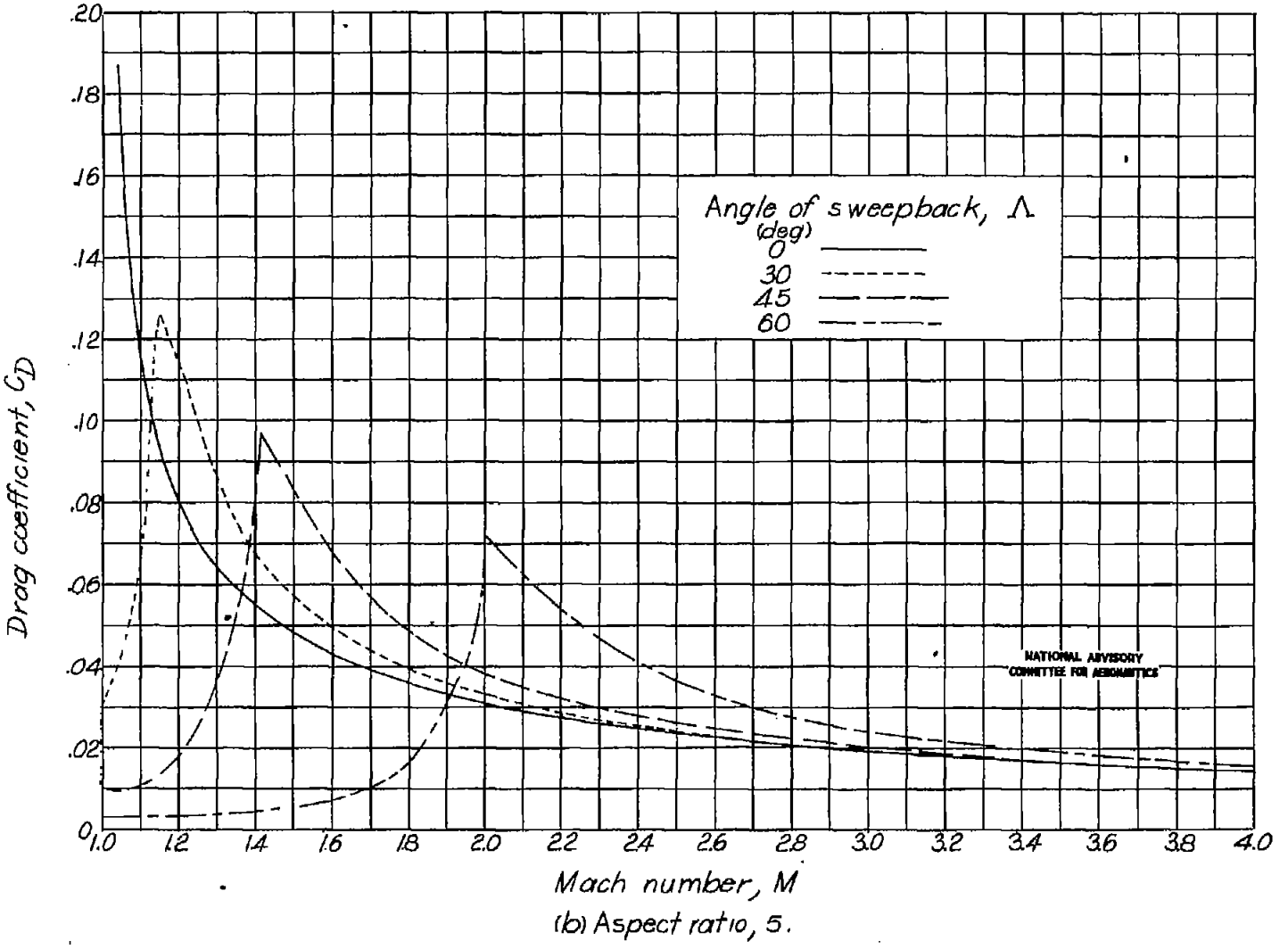

(b) Aspect ratio, 5.

Figure 10.- Concluded.